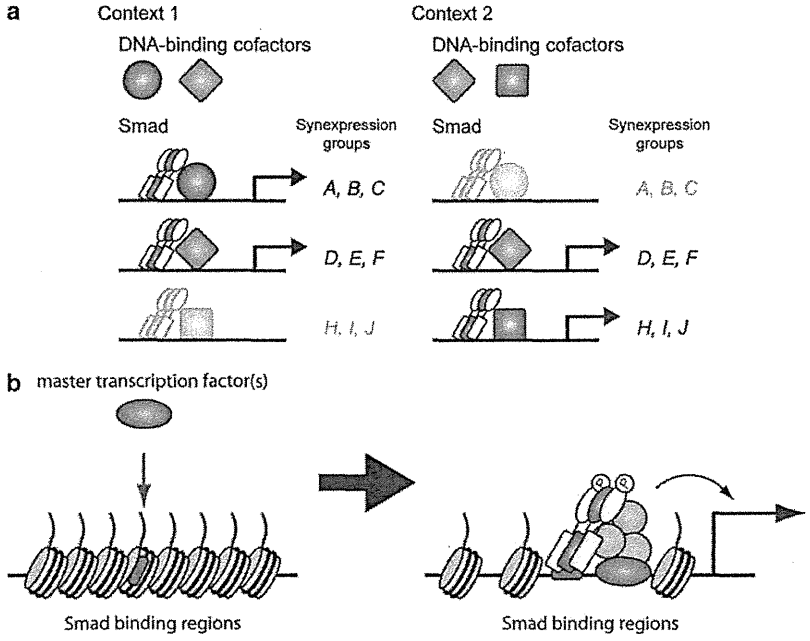

Figure 2. Factors that determine the binding patterns of Smads. (**a**) A group of genes that are simultaneously regulated by a specific Smad–cofactor complex is known as a synexpression group. Distinct combinations of DNA-binding cofactors in different contexts determine the set of genes regulated by Smad complexes. (**b**) Cell-type- or lineage-specific master transcription factors (purple) open up local chromatin structure to make Smad-binding regions (red) accessible. The master transcription factors also physically interact with Smads and, in some cases, recruit them to their binding sites. DNA-binding cofactors, induced and activated in context-dependent manner, strengthen the interaction between Smad and DNA. Interaction with coactivators/corepressors also affects the regulation of their target genes. A full colour version of this figure is available at the *Oncogene* journal online.

the BMP4-modulated early neural differentiation regulators, suggesting that loss of repressive histone marks through the Smad–KDM6B pathway explains the transcriptional regulation especially at later time points.

In addition to sequence-specific DNA-binding transcription factors, histone code reader proteins, which are recruited and bound to specific histone modifications, are reported to help to determine the binding sites of Smad proteins. Massagué and colleagues have reported that tripartite motif 33 (TRIM33, also known as TIF1γ or Ectodermin), physically interacts with Smad2 and Smad3, to make a TRIM33–Smad2/3 complex without Smad4.[69] The TRIM33 contains an N-terminal RING finger/B-box/coiled coil (RBCC) or TRIM domain, and a plant homeodomain (PHD) zinc finger and a Bromo domain in the C-terminus. They reported that the PHD-Bromo cassette recognized histone H3 lysine-9 trimethylation (H3K9me3) and H3 acetylation especially at lysine residues 18 and 23 (H3K18ac and H3K23ac). During mESC differentiation, nodal signaling triggered TRIM33–Smad2/3 complex formation. The TRIM33–Smad2/3 complex recognizes and binds to H3K9me3-K18ac dual histone marks and displaces the chromatin-compacting factor heterochromatin protein 1γ (HP1γ) in the *GSC* and *MIXL1* promoters, resulting in the remodeling of the local chromatin structure (Figure 3b).[70] Agricola *et al.*[71] also found that TRIM33 recognizes and binds to H3K18ac/K23ac. On the other hand, TRIM33 has been reported to bind Smad4 and function as a RING-type ubiquitin ligase for Smad4.[72] Consistent with this model, Agricola *et al.*[71] reported that TRIM33 inhibits Smad4 function through ubiquitin-mediated degradation of Smad4, and that its E3 ubiquitin ligase activity is induced after binding to histones. The detailed mechanisms have not been settled, but TRIM33 recognizes a specific histone code and modulates TGF-β/BMP signaling. Since the relationship between Smad proteins and histone modification marks has not been fully elucidated on a genome-wide scale, future analyses will address a possible mechanistic link between Smad proteins and epigenetic marks using ChIP-chip/ChIP-seq approach.

SMAD BINDING AND GENE REGULATION

Previous studies have indicated that binding of transcription factors detected by ChIP-chip/ChIP-seq experiments are not necessarily associated with transcriptional regulation of nearby genes (reviewed in Farnham[73]). It has frequently been observed that changing the level of a DNA-binding transcription factor alters the expression level of only 1–10% of its potential target genes. Most of the recent studies have confirmed that 1–20% of Smad-binding sites are associated with the regulation of expression of nearby genes. This discrepancy is in part due to the fact that mRNA levels do not only reflect transcriptional activities, since mRNA levels are also regulated by other biological processes, for example, degradation. Another explanation for the discrepancy is related to the definition of target genes. Although most studies assign binding sites to the nearest gene within 50 kb, this is not always the case. For example, Trompouki *et al.* revealed that several transcription factors, including Smad1, cooperatively regulate the expression of the hematopoietic gene *LMO2* through binding to the known enhancer region at 72 kb upstream of the transcription start site in K562 cells.[19,74] We also observed that Smad1/5 bound to a region 57 kb upstream of the transcription start site of *Smad6* in ECs, as well as the *LMO2* − 72 kb enhancer.[57] This region has been reported to be associated with Smad6 expression in the heart, vasculature and hematopoietic organs,[75] suggesting that the binding to this region, as well as the promoter region, plays an important role in these cell types. Recently, methods that characterize the chromatin architecture have been developed. Chromosome conformation capture (3C) assays make

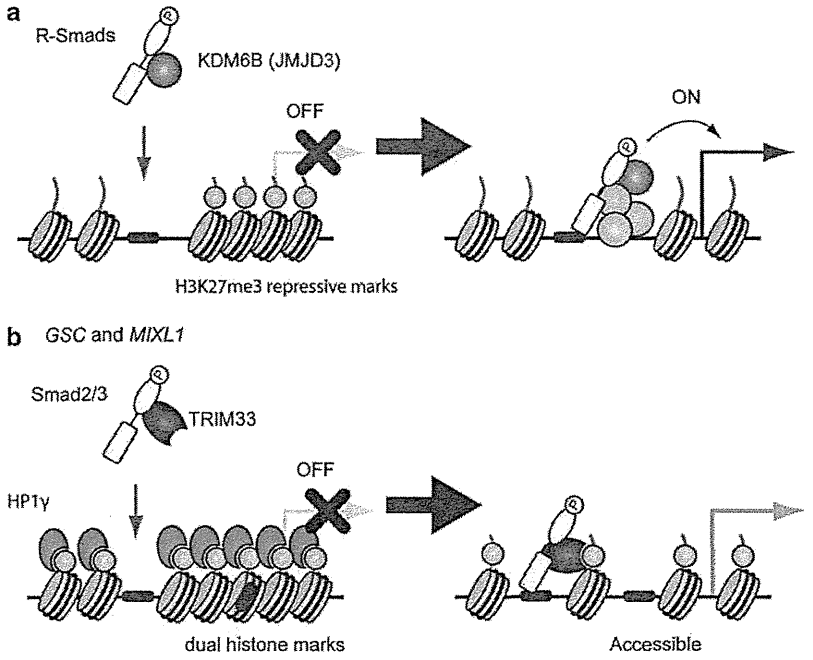

Figure 3. Smad proteins and histone modification marks. Smad proteins have been reported to induce local chromatin remodeling and modification at their binding sites. Several models are described in ES cells, where early developmental genes are poised and ready to be activated in response to extracellular signals, such as nodal. (**a**) R-Smads physically interact with a histone demethylase, KDM6B (also known as JMJD3), and recruit it to their target sites, followed by the loss of the H3K27me3 repressive mark (light green). (**b**) Xi *et al.*[70] reported that nodal signaling triggered TRIM33–Smad2/3 complex formation. The TRIM33–Smad2/3 complex recognizes and binds to H3K9me3-K18ac dual histone marks (light blue) and displaces the chromatin-compacting factor HP1γ (heterochromatin protein 1γ) in the *GSC* and *MIXL1* promoters, resulting in the remodeling of the local chromatin structure to make Smad-binding region(s) (red) accessible. A full colour version of this figure is available at the *Oncogene* journal online.

it possible to study long-distance regulation of genes by enhancers through formation of chromatin loops (reviewed in Simonis *et al.*[76]). Application of these technologies will help to identify the functional relationship between Smad-binding sites and genes implicated in cancer progression.

It is also possible that for many sites, binding of Smads is not sufficient for transcriptional regulation, but additional stimuli are required to drive the expression of the target genes. For example, costimulation with tumor necrosis factor-α, which induces the transcriptional repressor ATF-3, affects the expression regulation of the *Id1* gene and cellular response.[34,35] Sometimes, ligand stimulation itself induces these cofactors and makes a feed-forward circuit, like in myotube differentiation. The myogenic transcription factor MyoD directly regulates genes expressed during skeletal muscle differentiation together with other transcription factors such as MEF2[77] and Zfp238 (also known as RP58).[78] These transcription factors are also induced by MyoD, and MEF2 functions with MyoD in a positive feed-forward circuit,[77] while Zfp238 participates in a negative feed-forward circuit.[78] Comparison of MyoD-binding patterns of mouse C2C12 myoblasts and differentiated myotubes has revealed that most binding events in myoblasts are not directly associated with gene regulation. However, MyoD binding increases during myogenic differentiation at many of the regulatory regions associated with genes expressed in skeletal muscle. Intriguingly, the myotube-increased binding sites are enriched for MEF2-like motifs, while the myotube-decreased peaks are enriched for Zfp238-like motifs,[59] consistent with the fact that MEF2 positively and Zfp238 negatively cooperate with MyoD. It is possible that TGF-β stimulation induces certain transcription factors, which take part in feed-forward regulatory loops and cooperatively regulate gene expression especially at late time points.

IDENTIFICATION OF A TGF-β GENE SIGNATURE

The notion of 'gene signature' comes from the early work on cancer classification and prognosis prediction using genome-wide gene expression profiles obtained from microarray analyses of cancer patients.[79] Identification of a group of genes that reflect the activity of a common function, pathway or other property in a specific context, are sometimes more revealing compared with the analysis of single genes. Gene expression signatures obtained in experimental conditions has proved to subcategorize patients and predict their prognosis. Concerning TGF-β, Coulouarn *et al.*[80] reported that TGF-β-responsive genes at late time points, or a late TGF-β signature, which were identified in mouse primary hepatocytes, successfully discriminate distinct subgroups of hepatocellular carcinoma and possess a predictive value for hepatocellular carcinoma patients.

Combination of ChIP-chip/ChIP-seq and genome-wide transcriptome analyses provides an accurate prediction of target genes of Smad proteins. TGF-β family members regulate a variety of target genes both directly and indirectly, and modulate many biological processes. The chromatin-binding landscape of Smad proteins, obtained by ChIP-chip/ChIP-seq, will help to identify specific genes that are directly regulated by Smad proteins. It will also help to dissect a specific cellular program regulated by TGF-β family members, for example, the growth inhibitory and apoptosis programs of TGF-β. So far, many groups have identified groups of direct TGF-β target genes by using this strategy. Importantly, the TGF-β/Smad4 target gene signature identified in an ovarian cancer cell line predicts patient survival, based on *in silico* mining of publically available patient data bases.[21] Since TGF-β functions as a tumor suppressor in low-grade carcinoma cells, while it promotes metastasis in advanced carcinoma cells, a direct

comparison of the Smad-binding sites of these two stages of tumorigenesis, obtained from experimental models or from cancer patients, may reveal specific gene signatures of TGF-β correlating to its tumor suppressive and tumor-promoting roles, respectively. This may provide us more novel predictive indicators and biomarkers for TGF-β targeting treatments.

CONCLUSIONS AND PERSPECTIVES

The signaling pathways of TGF-β family members are key players in tumorigenesis and cancer progression. TGF-β can function both as a tumor-suppressing and a tumor-promoting factor during cancer progression. BMP signaling has been reported to play critical roles in oncogene-induced senescence, which is part of the tumorigenesis barrier and blocks cellular proliferation by inducing irreversible growth arrest.[66] Interestingly, BMP signaling induces differentiation of certain cancer-initiating cells, such as glioma-initiating cells,[81] while TGF-β/activin signaling maintains their stem cell-like properties.[9,10] Since Smad proteins are central mediators of the signal transduction, studies on global and genome-wide binding sites of Smad proteins may reveal important insights into their complex biological functions.

Identification of an appropriate antibody is the first and most important step for ChIP-chip and ChIP-seq analyses, because the quality of ChIP data depends crucially on the quality of the antibody used.[16] Since MH1 and MH2 domains are conserved among R-Smads, several specific antibodies for Smad proteins recognize their linker region. However, linker regions are targets of posttranslational modification and protein interactions, as discussed above. It is possible that such changes may attenuate the affinities of antibodies under specific conditions. Although ChIP-grade antibodies for Smad proteins have been established (Supplementary Table 2), careful interpretation of the results will be required.

In summary, genome-wide analysis of the binding sites of Smad proteins have led to important discoveries of their cell-type-specific and context-dependent functions. Application of genome-wide techniques to experimental models and human samples derived from cancer patients, will help to clarify their complex mechanisms during cancer progression, and may also provide potential prognostic biomarkers for future cancer therapy.

CONFLICT OF INTEREST

The authors declare no conflict of interest.

ACKNOWLEDGEMENTS

This work was supported by a grant from Swedish Cancer Society (Grant number 100452); KAKENHI (grants-in-aid for scientific research on Innovative Area (Integrative Research on Cancer Microenvironment Network; Grant number 22112002)) and for Young Scientists (B) (Grant numbers 22790750 (DK)); the Global Center of Excellence Program (Integrative Life Science Based on the Study of Biosignaling Mechanisms) from the Ministry of Education, Culture, Sports, Science and Technology (MEXT), Japan; a Research Grant from the Takeda Science Foundation and a Grant-in-Aid for Cancer Research for the Third-Term Comprehensive 10-Year Strategy for Cancer Control (H22-013) from the Ministry of Health, Labour and Welfare of Japan.

REFERENCES

1 Massague J. TGFbeta in cancer. *Cell* 2008; **134**: 215–230.
2 Ikushima H, Miyazono K. TGFbeta signalling: a complex web in cancer progression. *Nat Rev Cancer* 2010; **10**: 415–424.
3 Feng XH, Derynck R. Specificity and versatility in TGF-beta signaling through Smads. *Annu Rev Cell Dev Biol* 2005; **21**: 659–693.
4 Levy L, Hill CS. Alterations in components of the TGF-beta superfamily signaling pathways in human cancer. *Cytokine Growth Factor Rev* 2006; **17**: 41–58.
5 Yoshimura A, Wakabayashi Y, Mori T. Cellular and molecular basis for the regulation of inflammation by TGF-beta. *J Biochem* 2010; **147**: 781–792.
6 Roberts AB, Wakefield LM. The two faces of transforming growth factor beta in carcinogenesis. *Proc Natl Acad Sci USA* 2003; **100**: 8621–8623.
7 Moustakas A, Heldin CH. Non-Smad TGF-beta signals. *J Cell Sci* 2005; **118**: 3573–3584.
8 Miyazono K, Ehata S, Koinuma D. Tumor-promoting functions of transforming growth factor-beta in progression of cancer. *Ups J Med Sci* 2012; **117**: 143–152.
9 Ikushima H, Todo T, Ino Y, Takahashi M, Miyazawa K, Miyazono K. Autocrine TGF-beta signaling maintains tumorigenicity of glioma-initiating cells through Sry-related HMG-box factors. *Cell Stem Cell* 2009; **5**: 504–514.
10 Penuelas S, Anido J, Prieto-Sanchez RM, Folch G, Barba I, Cuartas I *et al.* TGF-beta increases glioma-initiating cell self-renewal through the induction of LIF in human glioblastoma. *Cancer Cell* 2009; **15**: 315–327.
11 Mani SA, Guo W, Liao MJ, Eaton EN, Ayyanan A, Zhou AY *et al.* The epithelial-mesenchymal transition generates cells with properties of stem cells. *Cell* 2008; **133**: 704–715.
12 Lonardo E, Hermann PC, Mueller MT, Huber S, Balic A, Miranda-Lorenzo I *et al.* Nodal/Activin signaling drives self-renewal and tumorigenicity of pancreatic cancer stem cells and provides a target for combined drug therapy. *Cell Stem Cell* 2011; **9**: 433–446.
13 Naka K, Hoshii T, Muraguchi T, Tadokoro Y, Ooshio T, Kondo Y *et al.* TGF-beta-FOXO signalling maintains leukaemia-initiating cells in chronic myeloid leukaemia. *Nature* 2010; **463**: 676–680.
14 Heldin CH, Miyazono K, ten Dijke P. TGF-beta signalling from cell membrane to nucleus through SMAD proteins. *Nature* 1997; **390**: 465–471.
15 Shi Y, Massague J. Mechanisms of TGF-beta signaling from cell membrane to the nucleus. *Cell* 2003; **113**: 685–700.
16 Park PJ. ChIP-seq: advantages and challenges of a maturing technology. *Nat Rev Genet* 2009; **10**: 669–680.
17 Pepke S, Wold B, Mortazavi A. Computation for ChIP-seq and RNA-seq studies. *Nat Methods* 2009; **6**: S22–S32.
18 Mullen AC, Orlando DA, Newman JJ, Loven J, Kumar RM, Bilodeau S *et al.* Master transcription factors determine cell-type-specific responses to TGF-beta signaling. *Cell* 2011; **147**: 565–576.
19 Trompouki E, Bowman TV, Lawton LN, Fan ZP, Wu DC, DiBiase A *et al.* Lineage regulators direct BMP and Wnt pathways to cell-specific programs during differentiation and regeneration. *Cell* 2011; **147**: 577–589.
20 Chen X, Xu H, Yuan P, Fang F, Huss M, Vega VB *et al.* Integration of external signaling pathways with the core transcriptional network in embryonic stem cells. *Cell* 2008; **133**: 1106–1117.
21 Kennedy BA, Deatherage DE, Gu F, Tang B, Chan MW, Nephew KP *et al.* ChIP-seq defined genome-wide map of TGFbeta/SMAD4 targets: implications with clinical outcome of ovarian cancer. *PLoS One* 2011; **6**: e22606.
22 Miyazono K, Kamiya Y, Morikawa M. Bone morphogenetic protein receptors and signal transduction. *J Biochem* 2010; **147**: 35–51.
23 Zhang Y, Feng XH, Smad3 Derynck R. and Smad4 cooperate with c-Jun/c-Fos to mediate TGF-beta-induced transcription. *Nature* 1998; **394**: 909–913.
24 Koinuma D, Tsutsumi S, Kamimura N, Taniguchi H, Miyazawa K, Sunamura M *et al.* Chromatin immunoprecipitation on microarray analysis of Smad2/3 binding sites reveals roles of ETS1 and TFAP2A in transforming growth factor beta signaling. *Mol Cell Biol* 2009; **29**: 172–186.
25 Koinuma D, Tsutsumi S, Kamimura N, Imamura T, Aburatani H, Miyazono K. Promoter-wide analysis of Smad4 binding sites in human epithelial cells. *Cancer Sci* 2009; **100**: 2133–2142.
26 Yoon SJ, Wills AE, Chuong E, Gupta R, HEB Baker JC. and E2A function as SMAD/FOXH1 cofactors. *Genes Dev* 2011; **25**: 1654–1661.
27 Ikushima H, Komuro A, Isogaya K, Shinozaki M, Hellman U, Miyazawa K *et al.* An Id-like molecule, HHM, is a synexpression group-restricted regulator of TGF-beta signalling. *EMBO J* 2008; **27**: 2955–2965.
28 Gomis RR, Alarcon C, Nadal C, Van Poznak C, Massague J. C/EBPbeta at the core of the TGFbeta cytostatic response and its evasion in metastatic breast cancer cells. *Cancer Cell* 2006; **10**: 203–214.
29 Silvestri C, Narimatsu M, von Both I, Liu Y, Tan NB, Izzi L *et al.* Genome-wide identification of Smad/Foxh1 targets reveals a role for Foxh1 in retinoic acid regulation and forebrain development. *Dev Cell* 2008; **14**: 411–423.
30 Kim SW, Yoon SJ, Chuong E, Oyolu C, Wills AE, Gupta R *et al.* Chromatin and transcriptional signatures for Nodal signaling during endoderm formation in hESCs. *Dev Biol* 2011; **357**: 492–504.
31 Gomis RR, Alarcon C, He W, Wang Q, Seoane J, Lash A *et al.* A FoxO-Smad synexpression group in human keratinocytes. *Proc Natl Acad Sci USA* 2006; **103**: 12747–12752.
32 Janknecht R, Wells NJ, Hunter T. TGF-beta-stimulated cooperation of smad proteins with the coactivators CBP/p300. *Genes Dev* 1998; **12**: 2114–2119.
33 Feng XH, Zhang Y, Wu RY, Derynck R. The tumor suppressor Smad4/DPC4 and transcriptional adaptor CBP/p300 are coactivators for smad3 in TGF-beta-induced transcriptional activation. *Genes Dev* 1998; **12**: 2153–2163.

34 Kang Y, Chen CR, Massague J. A self-enabling TGFbeta response coupled to stress signaling: Smad engages stress response factor ATF3 for Id1 repression in epithelial cells. *Mol Cell* 2003; **11**: 915–926.
35 Anido J, Saez-Borderias A, Gonzalez-Junca A, Rodon L, Folch G, Carmona MA *et al.* TGF-beta receptor inhibitors target the CD44(high)/Id1(high) glioma-initiating cell population in human glioblastoma. *Cancer Cell* 2010; **18**: 655–668.
36 Alarcon C, Zaromytidou AI, Xi Q, Gao S, Yu J, Fujisawa S *et al.* Nuclear CDKs drive Smad transcriptional activation and turnover in BMP and TGF-beta pathways. *Cell* 2009; **139**: 757–769.
37 Sapkota G, Alarcon C, Spagnoli FM, Brivanlou AH, Massague J. Balancing BMP signaling through integrated inputs into the Smad1 linker. *Mol Cell* 2007; **25**: 441–454.
38 Kretzschmar M, Doody J, Massague J. Opposing BMP and EGF signalling pathways converge on the TGF-beta family mediator Smad1. *Nature* 1997; **389**: 618–622.
39 Aubin J, Davy A, Soriano P. *In vivo* convergence of BMP and MAPK signaling pathways: impact of differential Smad1 phosphorylation on development and homeostasis. *Genes Dev* 2004; **18**: 1482–1494.
40 Fuentealba LC, Eivers E, Ikeda A, Hurtado C, Kuroda H, Pera EM *et al.* Integrating patterning signals: Wnt/GSK3 regulates the duration of the BMP/Smad1 signal. *Cell* 2007; **131**: 980–993.
41 Aragon E, Goerner N, Zaromytidou AI, Xi Q, Escobedo A, Massague J *et al.* A Smad action turnover switch operated by WW domain readers of a phosphoserine code. *Genes Dev* 2011; **25**: 1275–1288.
42 Zhu H, Kavsak P, Abdollah S, Wrana JL, Thomsen GHA. SMAD ubiquitin ligase targets the BMP pathway and affects embryonic pattern formation. *Nature* 1999; **400**: 687–693.
43 Kuratomi G, Komuro A, Goto K, Shinozaki M, Miyazawa K, Miyazono K *et al.* NEDD4-2 (neural precursor cell expressed, developmentally down-regulated 4-2) negatively regulates TGF-beta (transforming growth factor-beta) signalling by inducing ubiquitin-mediated degradation of Smad2 and TGF-beta type I receptor. *Biochem J* 2005; **386**: 461–470.
44 Gao S, Alarcon C, Sapkota G, Rahman S, Chen PY, Goerner N *et al.* Ubiquitin ligase Nedd4L targets activated Smad2/3 to limit TGF-beta signaling. *Mol Cell* 2009; **36**: 457–468.
45 Dupont S, Mamidi A, Cordenonsi M, Montagner M, Zacchigna L, Adorno M *et al.* FAM/USP9x, a deubiquitinating enzyme essential for TGFbeta signaling, controls Smad4 monoubiquitination. *Cell* 2009; **136**: 123–135.
46 Inui M, Manfrin A, Mamidi A, Martello G, Morsut L, Soligo S *et al.* USP15 is a deubiquitylating enzyme for receptor-activated SMADs. *Nat Cell Biol* 2011; **13**: 1368–1375.
47 Lonn P, van der Heide LP, Dahl M, Hellman U, Heldin CH, Moustakas A. PARP-1 attenuates Smad-mediated transcription. *Mol Cell* 2010; **40**: 521–532.
48 Huang D, Wang Y, Wang L, Zhang F, Deng S, Wang R *et al.* Poly(ADP-ribose) polymerase 1 is indispensable for transforming growth factor-beta Induced Smad3 activation in vascular smooth muscle cell. *PLoS One* 2011; **6**: e27123.
49 Zawel L, Dai JL, Buckhaults P, Zhou S, Kinzler KW, Vogelstein B *et al.* Human Smad3 and Smad4 are sequence-specific transcription activators. *Mol Cell* 1998; **1**: 611–617.
50 Yagi K, Goto D, Hamamoto T, Takenoshita S, Kato M, Miyazono K. Alternatively spliced variant of Smad2 lacking exon 3. Comparison with wild-type Smad2 and Smad3. *J Biol Chem* 1999; **274**: 703–709.
51 Chai J, Wu JW, Yan N, Massague J, Pavletich NP, Shi Y. Features of a Smad3 MH1-DNA complex. Roles of water and zinc in DNA binding. *J Biol Chem* 2003; **278**: 20327–20331.
52 Shi Y, Wang YF, Jayaraman L, Yang H, Massague J, Pavletich NP. Crystal structure of a Smad MH1 domain bound to DNA: insights on DNA binding in TGF-beta signaling. *Cell* 1998; **94**: 585–594.
53 BabuRajendran N, Palasingam P, Narasimhan K, Sun W, Prabhakar S, Jauch R *et al.* Structure of Smad1 MH1/DNA complex reveals distinctive rearrangements of BMP and TGF-beta effectors. *Nucleic Acids Res* 2010; **38**: 3477–3488.
54 Lee KL, Lim SK, Orlov YL, Yit le Y, Yang H, Ang LT *et al.* Graded Nodal/Activin signaling titrates conversion of quantitative phospho-Smad2 levels into qualitative embryonic stem cell fate decisions. *PLoS Genet* 2011; **7**: e1002130.
55 Zhang Y, Handley D, Kaplan T, Yu H, Bais AS, Richards T *et al.* High throughput determination of TGFbeta1/SMAD3 targets in A549 lung epithelial cells. *PLoS One* 2011; **6**: e20319.
56 Kim J, Johnson K, Chen HJ, Carroll S, Laughon A. Drosophila Mad binds to DNA and directly mediates activation of vestigial by Decapentaplegic. *Nature* 1997; **388**: 304–308.
57 Morikawa M, Koinuma D, Tsutsumi S, Vasilaki E, Kanki Y, Heldin CH *et al.* ChIP-seq reveals cell type-specific binding patterns of BMP-specific Smads and a novel binding motif. *Nucleic Acids Res* 2011; **39**: 8712–8727.
58 Mizutani A, Koinuma D, Tsutsumi S, Kamimura N, Morikawa M, Suzuki HI *et al.* Cell type-specific target selection by combinatorial binding of Smad2/3 proteins and hepatocyte nuclear factor 4alpha in HepG2 cells. *J Biol Chem* 2011; **286**: 29848–29860.
59 Cao Y, Yao Z, Sarkar D, Lawrence M, Sanchez GJ, Parker MH *et al.* Genome-wide MyoD binding in skeletal muscle cells: a potential for broad cellular reprogramming. *Dev Cell* 2010; **18**: 662–674.
60 Heinz S, Benner C, Spann N, Bertolino E, Lin YC, Laslo P *et al.* Simple combinations of lineage-determining transcription factors prime cis-regulatory elements required for macrophage and B cell identities. *Mol Cell* 2010; **38**: 576–589.
61 John S, Sabo PJ, Thurman RE, Sung MH, Biddie SC, Johnson TA *et al.* Chromatin accessibility pre-determines glucocorticoid receptor binding patterns. *Nat Genet* 2011; **43**: 264–268.
62 Zaret KS, Carroll JS. Pioneer transcription factors: establishing competence for gene expression. *Genes Dev* 2011; **25**: 2227–2241.
63 Harvey SA, Smith JC. Visualisation and quantification of morphogen gradient formation in the zebrafish. *PLoS Biol* 2009; **7**: e1000101.
64 Green JB, New HV, Smith JC. Responses of embryonic Xenopus cells to activin and FGF are separated by multiple dose thresholds and correspond to distinct axes of the mesoderm. *Cell* 1992; **71**: 731–739.
65 Fei T, Xia K, Li Z, Zhou B, Zhu S, Chen H *et al.* Genome-wide mapping of SMAD target genes reveals the role of BMP signaling in embryonic stem cell fate determination. *Genome Res* 2010; **20**: 36–44.
66 Kaneda A, Fujita T, Anai M, Yamamoto S, Nagae G, Morikawa M *et al.* Activation of Bmp2-Smad1 signal and its regulation by coordinated alteration of H3K27 trimethylation in Ras-induced senescence. *PLoS Genet* 2011; **7**: e1002359.
67 Akizu N, Estaras C, Guerrero L, Marti E, Martinez-Balbas MA. H3K27me3 regulates BMP activity in developing spinal cord. *Development* 2010; **137**: 2915–2925.
68 Dahle O, Kumar A, Kuehn MR. Nodal signaling recruits the histone demethylase Jmjd3 to counteract polycomb-mediated repression at target genes. *Sci Signal* 2010; **3**: ra48.
69 He W, Dorn DC, Erdjument-Bromage H, Tempst P, Moore MA, Massague J. Hematopoiesis controlled by distinct TIF1gamma and Smad4 branches of the TGFbeta pathway. *Cell* 2006; **125**: 929–941.
70 Xi Q, Wang Z, Zaromytidou AI, Zhang XH, Chow-Tsang LF, Liu JX *et al.* A poised chromatin platform for TGF-beta access to master regulators. *Cell* 2011; **147**: 1511–1524.
71 Agricola E, Randall RA, Gaarenstroom T, Dupont S, Hill CS. Recruitment of TIF1gamma to chromatin via its PHD finger-bromodomain activates its ubiquitin ligase and transcriptional repressor activities. *Mol Cell* 2011; **43**: 85–96.
72 Dupont S, Zacchigna L, Cordenonsi M, Soligo S, Adorno M, Rugge M *et al.* Germ-layer specification and control of cell growth by Ectodermin, a Smad4 ubiquitin ligase. *Cell* 2005; **121**: 87–99.
73 Farnham PJ. Insights from genomic profiling of transcription factors. *Nat Rev Genet* 2009; **10**: 605–616.
74 Landry JR, Bonadies N, Kinston S, Knezevic K, Wilson NK, Oram SH *et al.* Expression of the leukemia oncogene Lmo2 is controlled by an array of tissue-specific elements dispersed over 100 kb and bound by Tal1/Lmo2, Ets, and Gata factors. *Blood* 2009; **113**: 5783–5792.
75 Pimanda JE, Donaldson IJ, de Bruijn MF, Kinston S, Knezevic K, Huckle L *et al.* The SCL transcriptional network and BMP signaling pathway interact to regulate RUNX1 activity. *Proc Natl Acad Sci USA* 2007; **104**: 840–845.
76 Simonis M, Kooren J, de Laat W. An evaluation of 3C-based methods to capture DNA interactions. *Nat Methods* 2007; **4**: 895–901.
77 Penn BH, Bergstrom DA, Dilworth FJ, Bengal E, Tapscott SJ. A MyoD-generated feed-forward circuit temporally patterns gene expression during skeletal muscle differentiation. *Genes Dev* 2004; **18**: 2348–2353.
78 Yokoyama S, Ito Y, Ueno-Kudoh H, Shimizu H, Uchibe K, Albini S *et al.* A systems approach reveals that the myogenesis genome network is regulated by the transcriptional repressor RP58. *Dev Cell* 2009; **17**: 836–848.
79 van de Vijver MJ, He YD, van't Veer LJ, Dai H, Hart AA, Voskuil DW *et al.* A gene-expression signature as a predictor of survival in breast cancer. *N Engl J Med* 2002; **347**: 1999–2009.
80 Coulouarn C, Factor VM, Thorgeirsson SS. Transforming growth factor-beta gene expression signature in mouse hepatocytes predicts clinical outcome in human cancer. *Hepatology* 2008; **47**: 2059–2067.
81 Piccirillo SG, Reynolds BA, Zanetti N, Lamorte G, Binda E, Broggi G *et al.* Bone morphogenetic proteins inhibit the tumorigenic potential of human brain tumour-initiating cells. *Nature* 2006; **444**: 761–765.

Supplementary Information accompanies the paper on the Oncogene website (http://www.nature.com/onc)

Oncogene (2012), 1–10

www.nature.com/onc

ORIGINAL ARTICLE

Specific interactions between Smad proteins and AP-1 components determine TGFβ-induced breast cancer cell invasion

A Sundqvist[1], A Zieba[2,5], E Vasilaki[1,5], C Herrera Hidalgo[1], O Söderberg[2], D Koinuma[3], K Miyazono[1,3], C-H Heldin[1], U Landegren[2], P ten Dijke[1,4] and H van Dam[1,4]

Deregulation of the transforming growth factor β (TGFβ) signal transduction cascade is functionally linked to cancer. In early phases, TGFβ acts as a tumor suppressor by inhibiting tumor cell proliferation, whereas in late phases, it can act as a tumor promoter by stimulating tumor cell invasion and metastasis. Smad transcriptional effectors mediate TGFβ responses, but relatively little is known about the Smad-containing complexes that are important for epithelial–mesenchymal transition and invasion. In this study, we have tested the hypothesis that specific members of the AP-1 transcription factor family determine TGFβ signaling specificity in breast cancer cell invasion. Using a 3D model of collagen-embedded spheroids of MCF10A-MII premalignant human breast cancer cells, we identified the AP-1 transcription factor components c-Jun, JunB, c-Fos and Fra1 as essential factors for TGFβ-induced invasion and found that various mesenchymal and invasion-associated TGFβ-induced genes are co-regulated by these proteins. *In situ* proximity ligation assays showed that TGFβ signaling not only induces complexes between Smad3 and Smad4 in the nucleus but also complexes between Smad2/3 and Fra1, whereas complexes between Smad3, c-Jun and JunB could already be detected before TGFβ stimulation. Finally, chromatin immunoprecipitations showed that c-Jun, JunB and Fra1, but not c-Fos, are required for TGFβ-induced binding of Smad2/3 to the *mmp-10* and *pai-1* promoters. Together these results suggest that in particular formation of Smad2/3-Fra1 complexes may reflect activation of the Smad/AP-1-dependent TGFβ-induced invasion program.

Oncogene advance online publication, 27 August 2012; doi:10.1038/onc.2012.370

Keywords: invasion; spheroids; TGFβ; AP-1; Smad; PLA

INTRODUCTION

Transforming growth factor β (TGFβ) family members are secreted homodimeric proteins that exert a wide range of biological effects on a large variety of cell types, including regulation of proliferation, differentiation, migration and apoptosis. Signaling by TGFβ cytokines occurs via ligand-induced heteromeric complex formation of distinct type I and type II serine/threonine kinase receptors, causing the type I receptor to become phosphorylated by the constitutively active type II receptor. The activated TGFβ type I receptor kinase propagates the signal within the cell through phosphorylation of the receptor-regulated (R-)Smad proteins Smad2 and Smad3 at their extreme carboxyl-terminal serine residues.[1,2] The activated R-Smads then form heteromeric complexes with the common-partner (Co-)Smad, Smad4, and accumulate in the nucleus, where they can bind DNA and regulate gene expression. The Smads control gene expression in a cell type-specific manner by interacting with other proteins, such as AP-1, AP-2 and Ets transcription factors and specific co-activators and co-repressors.[3–7] These interactions can alter the intensity, duration and specificity of the TGFβ-signaling response.

Aberrant regulation of TGFβ signaling has been implicated in several pathological situations such as carcinogenesis, vascular disorders and fibrosis.[6,8] TGFβ has a biphasic role in tumor progression. In the early stages of tumor development, TGFβ inhibits cell growth and thus acts as a tumor suppressor. Escape from TGFβ/Smad-induced growth inhibition and apoptosis is commonly observed in tumors. In late-stage cancer, TGFβ has been shown to function as a tumor promoter, by stimulating dedifferentiation of epithelial cells to malignant invasive and metastatic fibroblastic cells.[6,9] This epithelial–mesenchymal transition (EMT) is a complex process. It involves disruption of polarization of epithelial cells and gain of spindle-shaped morphology with formation of actin stress fibers, reduced cell–cell junctions through delocalization and downregulation of E-cadherin, and increased cellular motility. Transcriptional repressors of E-cadherin, such as SIP1, Snail and Slug, are induced by TGFβ.[9–11] Induction of EMT by TGFβ can be observed in many different epithelial cell types and is promoted by activated Ras, activated Raf or by serum treatment.[12] It can be mediated both by perturbed Smad-dependent pathways and non-Smad signaling pathways, including MAP kinase pathways.[13,14] Knockdown of Smad3 and Smad4, but not of Smad2, inhibits TGFβ-induced EMT of NMuMG cells.[15,16]

The dimeric Jun/Fos and Jun/ATF AP-1 transcription factor complexes are composed of c-Jun, JunB, JunD, c-Fos, FosB, Fra1, Fra2 and certain ATF members, such as ATF2. These proteins control cell proliferation and differentiation by regulating gene expression in response to a wide range of stimuli, and they can be

[1]Ludwig Institute for Cancer Research, Science for Life Laboratory, Uppsala University, Uppsala, Sweden; [2]Department of Immunology, Genetics and Pathology, Science for Life Laboratory, Rudbeck Laboratory, Uppsala University, Uppsala, Sweden; [3]Department of Molecular Pathology, Graduate School of Medicine, University of Tokyo, Tokyo, Japan and [4]Department of Molecular Cell Biology, Centre for Biomedical Genetics, Leiden University Medical Center, Leiden, The Netherlands. Correspondence: Dr H van Dam, Department of Molecular Cell Biology, Centre for Biomedical Genetics, Leiden University Medical Center, PO Box 9600, 2300 RC, Leiden, The Netherlands.
E-mail: vdam@lumc.nl
[5]These authors contributed equally to this work.
Received 3 April 2012; revised 11 June 2012; accepted 9 July 2012

induced and/or activated through multiple signaling pathways, for example, MAP kinase pathways.[17–20] Certain AP-1 components have been implicated in carcinogenesis and tumor cell invasion.[20–23] In the case of TGFβ family signaling, both Smad-dependent and Smad-independent pathways can contribute to AP-1 activation.[4,14]

Previously, we established a 3D model of collagen-embedded spheroids of non-malignant, premalignant and metastatic MCF10A human breast cancer cells. We showed that in this system TGFβ-receptor I kinase and Smad4 and Smad3 are essential factors for TGFβ-induced invasion, by activating among others the secreted proteases MMP-2 and MMP-9.[24] In the present study, we have used this breast cancer invasion model to analyze the role of specific transcription factor AP-1 components in TGFβ/Smad-induced invasion.

RESULTS

TGFβ signaling induces increased levels of various AP-1 components in MCF10A MII cells

We previously showed that Smad4 and Smad3 have critical roles in TGFβ-induced invasion of both premalignant (MII) and malignant (MIV) MCF10A breast epithelial cells.[24] As Smads can regulate gene expression in cooperation with AP-1 transcription factors, and various AP-1 components have been implicated in tumor cell invasion, we first examined whether the expression of AP-1 components is regulated by TGFβ in MCF10A MII cells. As MII cells are Ras-transformed cells that can secrete various growth factors and cytokines themselves, including TGFβ and/or TGFβ-related cytokines,[24] we examined non-stimulated and TGFβ-stimulated cells both in the absence and presence of the TGFβRI kinase inhibitor SB-505124. Activation (phosphorylation) of Smad2 and Smad3 was analyzed for comparison.

We used TGFβ3 in this study because little is known about the response of breast cancer cells to TGFβ3, in contrast to TGFβ1. All three TGFβ isoforms are expressed during breast cancer progression, but some contradictory results have been obtained with respect to the correlation between expression levels and prognosis (reviewed in Laverty *et al.*[25]). Importantly, both TGFβ1 and TGFβ3 can bind directly to the type II receptor (TGFβRII), whereas TGF-β2 requires the presence of the co-receptor β-glycan. Moreover, we found the binding pattern of TGFβ3 in M2 cells to closely match the pattern reported for TGFβ1, binding TGFβRII, ALK5/TGFβRI and β-glycan.[24–26] However, in certain assays TGFβ3 appears to be a slightly more potent stimulator than TGFβ1.[25]

As shown in Figure 1 and Supplementary Figure 1, we found TGFβ to strongly increase the protein levels of the AP-1 components c-Jun, JunB, c-Fos and FosB. The TGFβRI kinase inhibitor SB-505124 inhibited the induction of c-Jun, JunB, c-Fos and FosB by TGFβ only at later time points (6 and 16 h; Figure 1). However, phosphorylation of Smad2 and Smad3 by TGFβ was already efficiently inhibited by SB-505124 after 1 h. Therefore, the Jun and Fos induction detected at the 1-h time point is most likely due to non-TGFβRI kinase-dependent TGFβ signaling.[14] Fra1, Fra2 and ATF2 were easily detected in non-stimulated MII cells, but only minor effects on expression levels were recorded upon addition of TGFβ or TGFβRI kinase inhibitor. Finally, the increase in c-Fos and Fra2 in the non-treated cells detected after 16 h, which was weakly inhibited by SB-505124, was probably due to autocrine factors, some of which might be TGFβ related and/or dependent.

Differential effects of AP-1 components on MCF10A MII spheroid invasion

We next analyzed the role of AP-1 in TGFβ-induced collagen invasion of MII spheroids. For this purpose, we first specifically depleted AP-1 components with validated Dharmacon (VWR International AB, Stockholm, Sweden) smart-pool siRNAs (Figure 2a). Knockdown of individual AP-1 components had only minor effects on the other members, with the exception of c-Fos and Fra1 that were significantly decreased by knockdown of c-Jun or JunB. These effects of AP-1 proteins on other family members are most likely due to the fact that various AP-1 components are (auto-)regulated via AP-1-binding sites in their promoters, and the fact that Fos family members can be stabilized by dimerization to Jun family members.[18,20,27] The reduced c-Jun levels upon Smad4 knockdown in Figure 2a indicate that the late TGFβ induction of *c-jun* is Smad dependent, which is in line with previous studies.[4,14]

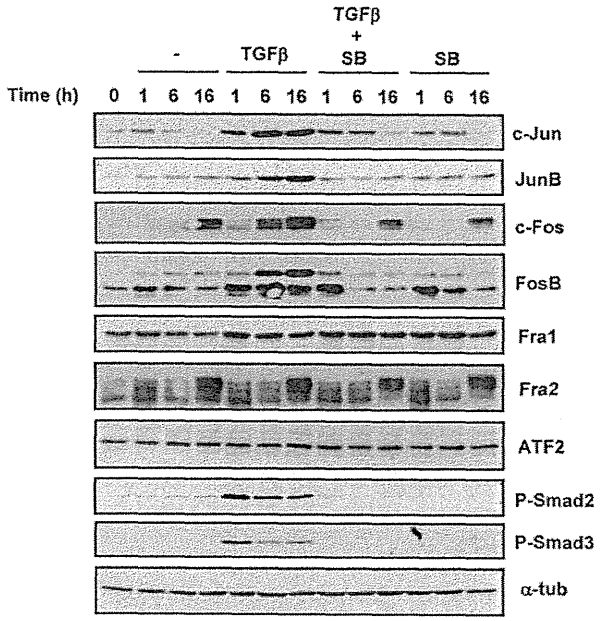

Figure 1. TGFβ-induced AP-1 activity in MCF10A MII cells. MCF10A MII cells were serum-starved for 16 h, treated with TGFβ3 and the TGFβRI inhibitor SB-505124 as indicated, and analyzed by immunoblotting. SB-505124 was added 15 min before TGFβ3.

The effect of AP-1 knockdown on invasion was subsequently compared with the effect of the TGFβRI-kinase inhibitor SB-505124 and Smad4 siRNA, as our previous studies had shown that TGFβRI-kinase inhibition nearly completely blocks TGFβ-induced collagen invasion of MII spheroids, whereas knockdown of Smad4 only has a partial effect.[24] Importantly, siRNA-mediated knockdown of none of the AP-1 components affected the formation of spheroids (Figure 2b). However, knockdown of JunB strongly inhibited TGFβ-induced collagen invasion, whereas knockdown of c-Jun, c-Fos and Fra1 inhibited invasion to a slightly lower extent (Figures 2c and d). Knockdown of ATF2, FosB or Fra2 not or hardly inhibited TGFβ-induced collagen invasion (Figures 2c and d). These results therefore suggest that the induction of c-Jun, JunB and c-Fos by TGFβ is an essential step during TGFβ-induced invasion of MII cells, and that only a specific subset of AP-1 components is essential.

Identification of Smad and AP-1-dependent mesenchymal and invasion-associated genes

We next tried to obtain clues on the mechanism by which AP-1 mediates TGFβ-induced invasion in MII cells. For this, we examined the effect of c-Jun, JunB, c-Fos or Fra1 knockdown on the expression of a panel of invasion- and EMT-associated TGFβ target genes. As shown in Figure 3a, c-Jun, JunB and Fra1, but

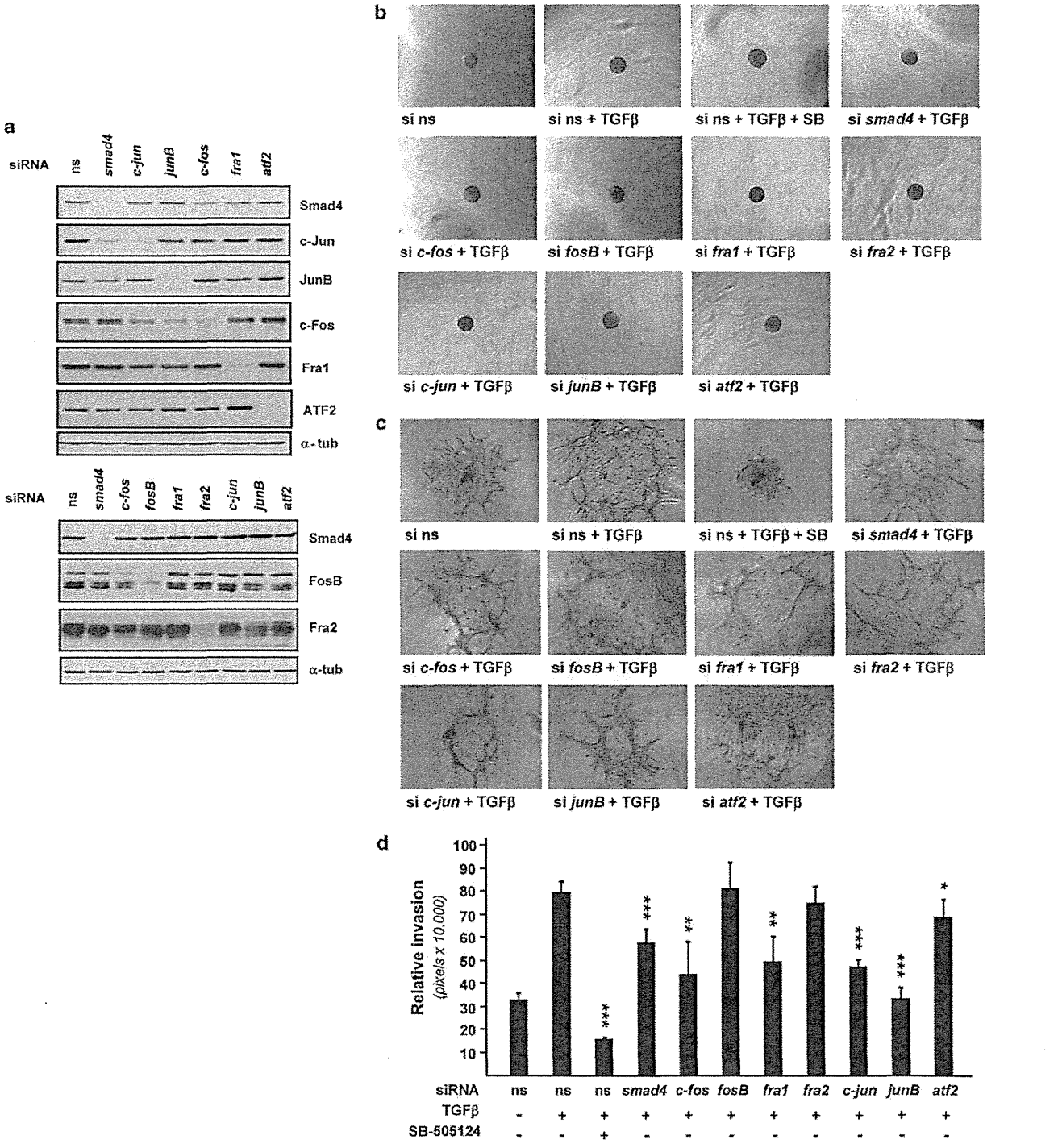

Figure 2. Effect of AP-1 knockdown on MCF10A MII spheroid invasion in collagen. (**a**) Knockdown of AP-1 components. After transfection with Dharmacon smart pool siRNAs, cells were stimulated with TGFβ3 for 19 h and analyzed by immunoblotting (ns: non-specific siRNA). (**b–d**) TGFβ-induced collagen invasion of MCF10A MII spheroids. Forty-eight hours after transfection with siRNA, cells were embedded in collagen in the absence or presence of TGFβ3 and the TGFβRI inhibitor SB-505124 (SB) as indicated. Representative pictures of spheroids were taken just after embedding into collagen (**b**) or 48 h after embedding (**c**). (**d**) Relative invasion was quantified as the mean area that the spheroids transfected with the individual siRNA occupy 48 h after being embedded in collagen. Results are expressed as mean ± s.d. ($n = 5$). $^{*}P < 0.05$, $^{**}P < 0.01$, $^{***}P < 0.001$.

not c-Fos, were found to be critical for the TGFβ-induced expression of *mmp-1*, *mmp-9* and *mmp-10*. However, TGFβ induction of *mmp-2* and *integrin* α_v was not at all or only minimally decreased by knockdown of these AP-1 components (Figures 3a and b). c-Jun and JunB were also found to contribute to TGFβ induction of *slug*, *uPAR* and *pai-1*, and both c-Fos and Fra1

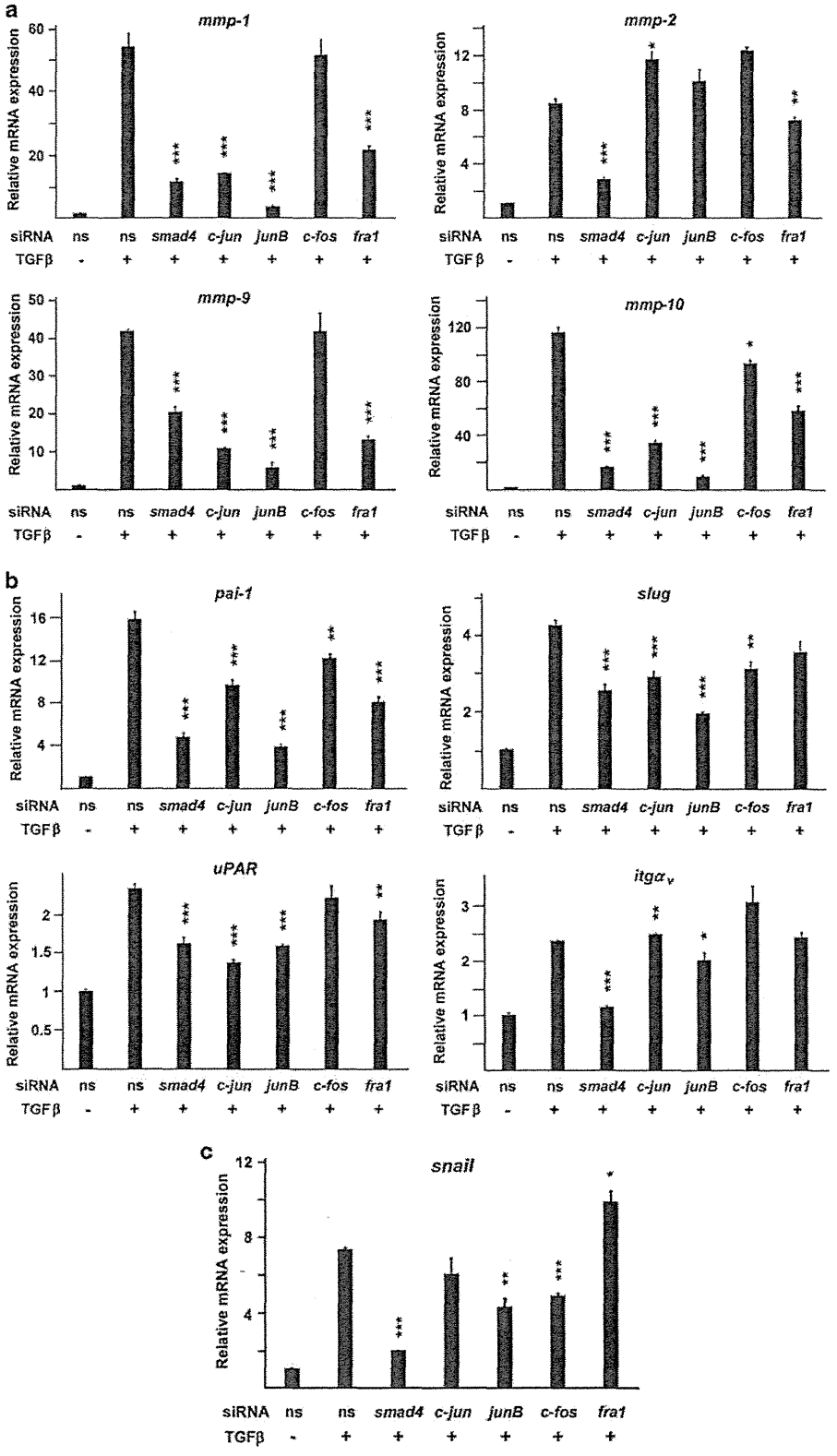

Figure 3. c-Jun, JunB, Fra1 and/or c-Fos regulate several TGFβ-induced EMT and invasion-related genes. (**a–c**) MCF10A MII cells were transfected with the indicated control (ns: non-specific) or specific siRNAs, serum-starved and stimulated for 19 h (**a**, **b**) or 70 min (**c**) with TGFβ3. mRNA levels were analyzed by qPCR and normalized to *gapdh*, which was not significantly affected by the treatments. Values and error bars represent the mean ± s.d. of triplicates and are representative of at least two independent experiments. $^{*}P<0.05$, $^{**}P<0.01$, $^{***}P<0.001$.

appeared to be involved in the induction of *slug* and *pai-1* (Figure 3b). In contrast, the induction of *snail* was dependent on c-Fos, but not on Fra1 (Figure 3c). All genes examined required Smad4 (Figures 3a–c). These results thus indicate that Jun/c-Fos and Jun/Fra1 complexes control distinct subsets of Smad4-dependent EMT and invasion-associated genes.

As TGFβ strongly enhanced the synthesis of c-Jun and JunB (Figure 1), we subsequently examined the effect of Jun overexpression on the expression of *mmp-1*, *-2* and *-10*. As shown in Figure 4a, transient transfection of c-Jun induced the expression of endogenous *mmp-1* and *-10* both with and without TGFβ treatment for 4 h. However, transfection of JunB only had a weak stimulatory effect on TGFβ-induced *mmp-10*, suggesting that enhanced levels of JunB by itself are not sufficient. The expression of *mmp-2* was somewhat inhibited by overexpressed c-Jun and JunB (Figure 4a), in line with the slight enhancement by the Jun knockdown in Figure 3a. As overexpressed Smad and Jun proteins were previously shown to be able to cooperatively activate Smad/AP-1-dependent reporter plasmids in the absence of TGFβ-stimulation,[3,4] we next overexpressed JunB together with Smad3 and 4. Like JunB, overexpressed Smad3 and 4 could not activate the endogenous *mmp-1* and *mmp-10* genes by themselves, although the TGFβ-inducible reporter plasmid CAGA-luciferase was efficiently induced under these conditions (data not shown). However, the combination of JunB, Smad3 and Smad4 induced these genes to the same extent as overexpression of c-Jun (see the fold activation in Figures 4a and b). These data further confirm that both c-Jun and JunB contribute to the TGFβ- and Smad-induced activation of specific *mmp* genes in MII cells.

In situ detection of Smad-AP-1 interaction by proximity ligation

Some Smad members and AP-1 components, for instance Smad3 and c-Jun, have been found to associate *in vitro* and/or upon overexpression.[3,4] To examine whether we could detect endogenous complexes between Smad proteins and AP-1 components

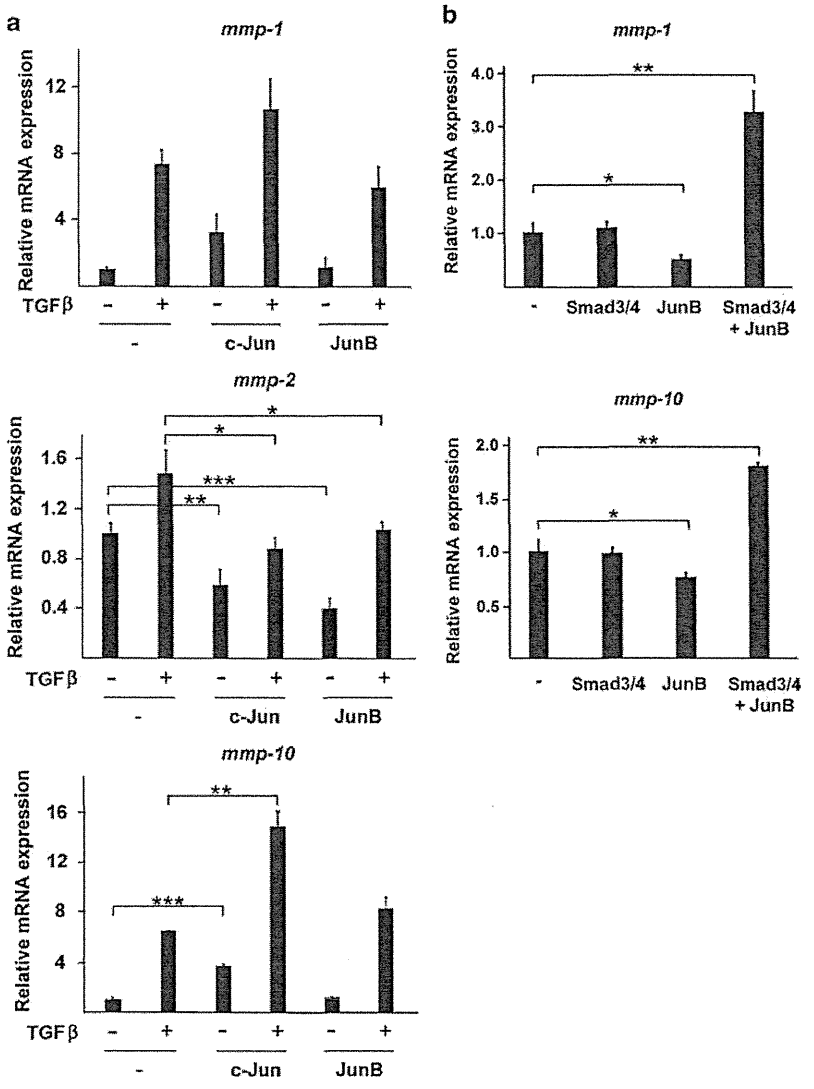

Figure 4. c-Jun and JunB differently affect Smad-dependent *mmp* genes. (**a**, **b**) MCF10A MII cells were transfected with expression vectors for c-Jun, JunB, Smad3 and/or Smad4, and/or stimulated with TGFβ for 4 h as indicated. mRNA levels were analyzed by qPCR and normalized to *gapdh*, which was not significantly affected by the treatments. Values and error bars represent the mean ± s.d. of triplicates and are representative of at least two independent experiments. $^{*}P<0.05$, $^{**}P<0.01$, $^{***}P<0.001$.

in MII cells *in situ*, we performed proximity ligation assays (PLA).[28,29] TGFβ treatment induced formation of nuclear complexes of Smad3 and Smad4, while nuclear complexes of c-Jun and Smad3, and—to a lesser extent—JunB and Smad3, were already present in non-stimulated cells, and only weakly increased upon TGFβ treatment (Figures 5a and c). We could not consistently detect complex formation between Smad4 and the Jun proteins under these conditions, and only detected very low levels of Smad2 binding to Smad4 and the AP-1 components in these cells (data not shown). Interactions between c-Jun and Fra1 and between JunB and Fra1 were clearly detectable in many but not all non-stimulated cells, and only c-Jun/Fra1 complexes were clearly increased by TGFβ (Figures 5b and c). Some c-Jun/c-Fos complexes were also already present in non-stimulated cells, but their levels were considerably higher after TGFβ stimulation. However, the strongest stimulatory effect of TGFβ was observed on the interaction between Smad2/3 and Fra1 (Figures 5b and c). (Note that we cannot rule out the presence of Smad2 in these complexes because the antibody used can recognize both Smad2 and Smad3.) In contrast, much less complexes were detected that contained Smad2/3 and c-Fos (Figures 5b and c). In the presence of the TGFβRI inhibitor SB-505124, TGFβ was unable to increase most of these Smad and AP-1 complexes (Figure 5c).

These results show that both c-Jun and JunB can interact with nuclear Smad3 in MII cells also in the absence of TGFβ stimulation, whereas the interaction between Smad2/3 and Fra1 seems to be efficiently enhanced upon activation of TGFβ signaling.

c-Jun, JunB and Fra1 enable TGFβ-induced binding of Smad2/3 to the *mmp-10* and *pai-1* promoters

TGFβ-induced binding of Smad2/3 to the promoters of TGFβ-target genes represents a critical step in TGFβ/Smad-induced gene activation.[5,6] To further elucidate the mechanism by which c-Jun, JunB, c-Fos and Fra1 mediate TGFβ-induced expression of invasion genes, we analyzed Smad2/3 promoter recruitment in MII cells in the absence and presence of these AP-1 components. As shown by the chromatin immunoprecipitations (ChIP) in Figure 6, the binding of Smad2/3 to the promoters of *mmp-10* and *pai-1* was efficiently increased by TGFβ treatment. As expected, knockdown of Smad4 strongly inhibited Smad2/3 binding. Importantly, knockdown of c-Jun, JunB and Fra1 also strongly reduced Smad2/3 binding to the *mmp-10* promoter, but knockdown of c-Fos did not. Moreover, both JunB and Fra1 were critical for Smad2/3 recruitment to the *pai-1* promoter. Together with the mRNA analysis and PLAs presented above, these results indicate that interactions involving Smad3, c-Jun, JunB and Fra1, but not c-Fos, are critical for the TGFβ-induced binding of Smad3 to AP-1-dependent TGFβ-induced invasion genes.

DISCUSSION

TGFβ signaling has a dual role in cancer. In the early stages of tumor development, it can inhibit carcinogenesis through TGFβ/Smad-induced growth inhibition and apoptosis. However, during later stages of cancer progression, TGFβ can promote tumor invasion and metastasis by inducing EMT and affecting the tumor stroma, thereby enhancing survival, motility and invasion of the tumor cell. To overcome the tumor-suppressive effect of the TGFβ pathway, the core components—including Smad2 and Smad4—are frequently inactivated in cancer tissue, for instance in colorectal cancer. However, breast cancers mainly exhibit defects in downstream mediators of the cytostatic action of TGFβ. They exhibit normal signaling from receptors to Smads and retain or gain other properties of TGFβ responsiveness, indicating that TGFβ/Smad signaling is critical for breast cancer progression.[30–36]

Induction of EMT and invasion by TGFβ is promoted by activated Ras, and can be mediated both via Smad-dependent pathways and non-Smad signaling such as by MAP kinase pathways.[9,12–14,37] As TGFβ, Ras and MAP kinases can activate transcription factor AP-1, we have in this study investigated which role the individual components of transcription factor AP-1 complexes play in TGFβ-induced breast cancer cell invasion. TGFβ was found to induce increased protein levels of c-Jun, JunB, c-Fos and FosB with prolonged kinetics (at least up to 16 h) in MCF10A-MII cells, whereas Fra1, Fra2 and ATF2 were efficiently expressed, but not or only slightly affected by TGFβ stimulation. The TGFβRI kinase inhibitor SB-505124 inhibited the induction of c-Jun, JunB, c-Fos and FosB only at the later time points, suggesting that the early activation is mediated by TGFβRI kinase-independent JNK/p38 activation.[14]

By using a validated siRNA approach, we could show that c-Jun, JunB, c-Fos or Fra1 are required for efficient TGFβ-induced invasion, whereas FosB and Fra2 did not contribute. It is important to note though that—in spite of their different transcriptional activities—c-Fos, FosB, Fra1 and Fra2 can all dimerize with the Jun proteins and share some critical functions in cell cycle control and mouse development.[17,19,38] Therefore, we cannot yet exclude that in the absence of c-Fos and/or Fra1 proteins, FosB and/or Fra2 may, to some extent, take over their functions in TGFβ-induced invasion. Similarly, c-Fos may take over some functions of Fra1 upon Fra1 depletion and vice versa. Interestingly, none of the siRNAs used inhibited the invasion to the same extent as the TGFRI-kinase inhibitor SB-505124. This could point to further redundancy within the Smad, Jun and Fos families, or to involvement of additional TGFβ-regulated and/or cooperating factors, such as Rho kinases and Ets transcription factors.[6,7,14]

We found that both c-Fos and Fra1 contribute to TGFβ-mediated induction of the mesenchymal and EMT-associated genes *pai-1* and *slug*, which supports the idea that these two Jun dimer-partners have (at least partially) overlapping functions in invasion. However, additional results showed that c-Fos and Fra1 also exhibit unique functions in the induction of EMT and invasion genes by TGFβ: only c-Fos was found to be required for efficient induction of snail, whereas only Fra1 was essential for the induction of *mmp-1* and *mmp-9*. The expression of *mmp-10* was also strongly dependent on the presence of Fra1, while c-Fos had limited effects. Moreover, ChIPs showed that Fra1 but not c-Fos is critical for the TGFβ-induced binding of Smad2/3 to the *pai-1* and *mmp-10* promoters, and with PLAs we could only efficiently detect TGFβ-induced complexes between Smad2/3 and Fra1. These results indicate that Fra1 rather than c-Fos is required for the recruitment of Smads to the Smad/AP-1 sites of these invasion-associated genes, whereas c-Fos may mainly act on *pai-1* via (Smad-independent) AP-1 sites. Interestingly, knockdown of c-Jun also did not affect Smad2/3 recruitment to *pai-1* (Figure 6), suggesting that both c-Jun and c-Fos activate *pai-1* in a Smad2/3-independent manner, in contrast to JunB and Fra1. In fact, c-Jun might also activate the *mmp-1* and *mmp-10* genes in part via a Smad-independent mechanism, as overexpression of c-Jun, but not of JunB, could activate these *mmp* genes in the absence of TGFβ stimulation or Smad3/4 overexpression (Figure 4a).

Previous studies in human cells and/or in mouse models showed that c-Fos and Fra1 can both have essential roles in EMT and tumor progression, thereby presumably participating in Jun/Fos trancription complexes binding to AP-1 sites in genes critical for EMT, survival and/or migration/invasion.[19,21–23,39,40] Whether some of these functions are mediated via interaction with Smad proteins is to our knowledge still unknown. However, it is important to mention here that TGFβ itself is an AP-1 target gene, indicating that AP-1 components are likely to control the persistence of TGFβ signaling at multiple levels.

In the absence of active TGFβRI, Smad proteins shuttle between the nucleus and cytoplasm, whereas AP-1 components are

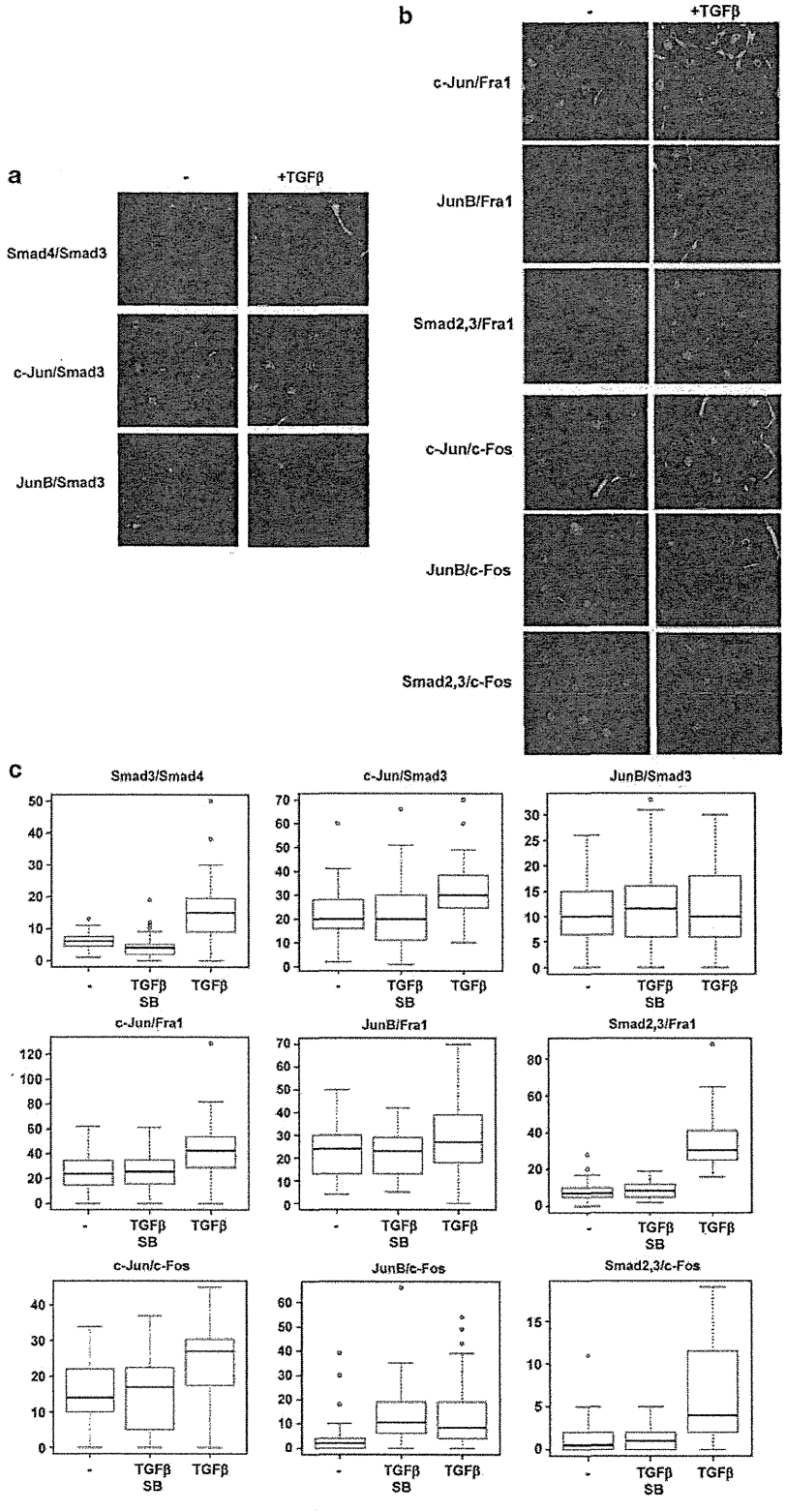

Figure 5. Effect of TGFβ on Smad/AP-1 complex formation in premalignant MCF10A cells. (**a**, **b**) *In situ* PLA in serum-starved MCF10A-MII cells treated for 1 h with TGFβ3 or not (−). Primary mouse and rabbit antibodies against the indicated Smad and AP-1 family members were combined with secondary PLA probes (Olink Bioscience). The interaction events are visible as red dots (nuclear staining in blue (Hoechst) and actin staining in green (FITC)). (**c**) Quantification of nuclear PLA signals (y axis) obtained for the indicated antibody combinations before and after 1 h treatment with TGFβ3 in the absence and presence of the TGFβRI inhibitor SB-505124 (SB). The box plots indicate the median and range of the detected signals.

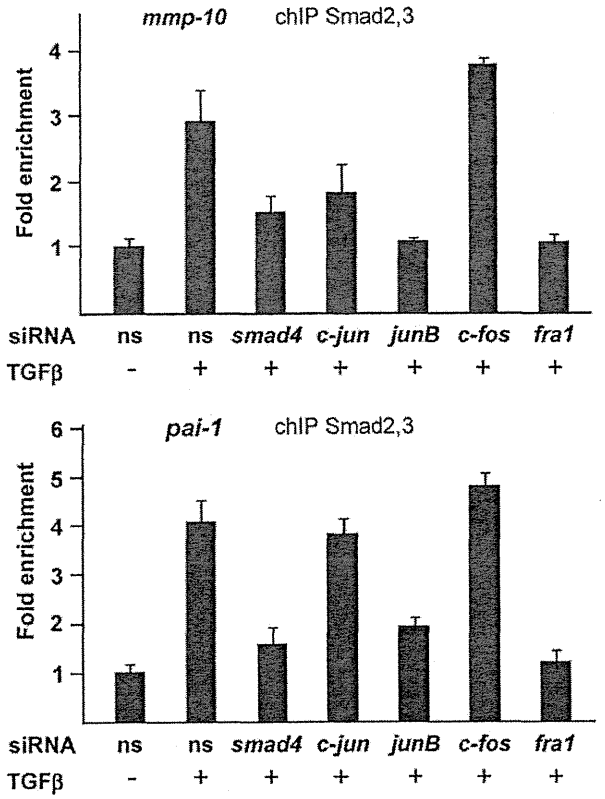

Figure 6. c-Jun, JunB and Fra1 determine Smad2/3 binding to the *mmp-10* and *pai-1* promoters. MCF10A MII cells were transfected with the indicated control (ns: non-specific) or specific siRNAs, serum-starved and stimulated for 16 h with TGFβ3. ChIP was performed with an antibody against Smad2, 3 and normalized to control IgG. The fold enrichment for non-stimulated control transfected cells was set at 1.0 for each gene.

(predominantly) located in the nucleus. Our PLAs showed that 1 h TGFβ treatment induces not only complexes between Smad3 and Smad4 in the nucleus but also complexes between Smad2/3 and Fra1, whereas complexes between Smad3, c-Jun and JunB could already be detected before TGFβ stimulation. At later time points after stimulation, when the levels of c-Jun and JunB are strongly increased, we also saw a stronger increase in Smad3/Jun complexes (our unpublished observations). These complexes might therefore further enhance Smad-AP-1-dependent TGFβ target genes and thus alter the intensity and duration, as well as the specificity of the Smad-signaling response. Moreover, in certain situations—such as in the case of *mmp-2* (Figure 4)—they might inhibit Smad-dependent transcription via off-DNA interactions.[4,41]

In summary, our results show that specific AP-1 members determine TGFβ signaling specificity in EMT and breast cancer cell invasion by functionally interacting with Smad factors. Our results further suggest that in particular formation of Smad2/3-Fra1 complexes may reflect activation of the Smad/AP-1-dependent TGFβ-induced invasion program. Previously, we found that aggressive basal-like breast cancer cells can be discriminated from much less invasive luminal-like cells by PLA detection of c-Jun/Fra1, rather than of c-Jun/ATF2 and c-Jun/c-Fos.[29] JunB/Fra1 dimers were also found to be increased in the aggressive cells (our unpublished observations). It will therefore be interesting to compare Smad/AP-1 complex formation in basal-like breast cancer cells versus luminal-like cells, and in biopsies of breast cancer patients.

MATERIALS AND METHODS

Cell culture

MCF10A MII cells were obtained from Dr Fred Miller (Barbara Ann Karmanos Cancer Institute, Detroit, MI, USA) and maintained at 37 °C and 5% CO_2 in DMEM/F12 (Gibco, Life Technologies Europe BV, Stockholm, Sweden) supplemented with 5% fetal bovine serum (Biowest, Biotech-IgG AB, Lund, Sweden), 20 ng/ml epidermal growth factor (Upstate, Millipore AB, Solna, Sweden), 100 ng/ml cholera toxin (Sigma, Sigma-Aldrich Sweden AB, Stockholm, Sweden), 0.5 μg/ml hydrocortisone (Sigma) and 10 μg/ml insulin (Sigma).

3D spheroid invasion assays

Semi-confluent cells were trypsinized, counted and re-suspended in medium containing 2.4 mg/ml methylcellulose (Sigma) at the concentration of 10^4 cells/ml. A 100-μl of suspension was added into each well of *U*-bottom 96-well plate allowing the formation of one spheroid per well. For siRNA-mediated knockdown, the trypsinized cells were incubated with specific smart-pool siRNAs obtained from Dharmacon according to the manufacturers procedure. All spheroids consisted of 10^3 cells. Two days after plating spheroids were harvested and embedded into collagen. Flat-bottom 96-well plates were coated with neutralized bovine collagen-I (PureCol, Advanced BioMatrix, Nutacon BV, Leimuiden, The Netherlands) according to manufacturer's protocol. Single spheroids were embedded in a 1:1 mix of neutralized collagen and medium supplemented with 12 mg/ml of methylcellulose. TGFβ3 (generous gift of Dr K Iwata, OSI Pharmaceuticals, Inc., New York, NY, USA) and/or SB-505124 (Sigma) were directly added to the embedding solution. Invasion was quantified by measuring the area occupied by cells at day 2 by using Adobe Photosphop CS3 software. Pictures were taken at day 0 and day 2 after embedding.

Western blot analysis

Five hundred thousand cells were seeded in 6-well plates. The following day, cells were starved 16 h in 0.2% FBS and stimulated with 5 ng/ml of TGF-β3 for indicated time points. SB-505124 was added 15 min before TGFβ. For siRNA transfection, On Target Plus pools of four oligonucleotides (Dharmacon) were transfected with DharmaFECT (Dharmacon) transfection reagent in 12-well plates according to manufacturer's instructions at 25 nM final concentration. Cells were lysed in 2 × SDS loading buffer and subjected to SDS–PAGE and western blotting. The following antibodies were used: anti-c-Jun (sc-1694; Santa Cruz Biotechnology, Santa Cruz, CA, USA), anti-JunB (sc-8051; Santa Cruz), anti-c-Fos (sc-52; Santa Cruz), anti-FosB (#2251; Cell Signaling Technology, BioNordika Sweden AB, Stockholm, Sweden), anti-Fra1(sc-22794; Santa Cruz), anti-Fra2 (sc-604; Santa Cruz), anti-ATF2 (sc-187; Santa Cruz), anti-phospho-Ser465/425 Smad2 (#3108; Cell Signaling Technology), anti-phospho-Ser423/425 Smad3 (#9520; Cell Signaling Technology), anti-Smad4 (sc-7966; Santa Cruz).

RNA isolation, cDNA synthesis and quantitative real time–PCR

Cells were treated as described for western analysis and total RNA was isolated by GeneJET RNA Purification Kit (Fermentas, Helsingborg, Sweden). cDNA was prepared by annealing 1 μg RNA with oligo dT as per manufacturer's instructions (RevertAid H Minus First Strand cDNA Synthesis Kit, Fermentas). The cDNA samples were diluted 10 times with water. A total of 2 μl of cDNA was used in 12 μl quantitative real time-PCR reactions with appropriate primers and Maxima SYBR Green qPCR MasterMix (Fermentas). All samples were analyzed in triplicate for each primer set. Gene expression levels were determined with the comparative ΔC_t method and the non-stimulated condition was set to 1. Relative expression levels are presented as mean ± s.d. Statistical significance was determined by unpaired Student's two-tailed *t*-test. $P<0.05$ was considered as statistically significant. The complete primers list can be found in the Supplementary Table S1.

Proximity ligation assay

Cells were seeded on tissue culture-treated chamber slides (REF 354108; BD Falcon, BD Biosciences, BD AB, Stockholm, Sweden). The following day, cells were starved 16 h in 0.2% FBS and stimulated with 5 ng/ml of TGFβ3 for 1 h. Cells were fixed as described previously.[29] The slides

were then blocked in 5% donkey serum (Jackson Immunoscience, Jackson ImmunoResearch Europe Ltd, Suffolk, UK), 2 μg/ml salmon sperm (Sigma), 5 mg/ml bovine serum albumin (Sigma) and 2 mM cysteine (Sigma) in TBS-Tween with 5 mM EDTA (Sigma) for 1 h and incubated overnight at 4 °C with appropriate combinations of mouse and rabbit antibodies diluted 1:50 in blocking solution. After washing, the slides were incubated with Duolink PLA Rabbit MINUS and PLA Mouse PLUS proximity probes (Olink Bioscience, Uppsala, Sweden) and proximity ligation was performed using the Duolink detection reagent kit (Olink Bioscience) according to the manufacturers protocol. Fluorescence was detected using a Zeiss AxioPlan2 microscope with a ×20/0.8 Plan-Apo objective. Images were acquired with an Axiocam MRm camera and AxioVision Rel. 4.8 software (Carl Zeiss AB, Stockholm, Sweden) as sets of color-images and prepared using Adobe Photoshop CS5 software. The DuolinkImageTool software was used for image analysis. Fluorescent signals from RCA products were defined and counted per cell with distinction of the nucleus and the cytoplasm. For each experiment, signals from 150 to 200 cells were quantified. Antibodies used for PLA were: mouse anti-Smad4 (sc-7966; Santa Cruz), rabbit anti-Smad3 (EP784Y; Epitomics, Nordic BioSite AB, Täby, Sweden), mouse anti-c-Jun #2315 (Cell Signaling Technology), mouse anti-JunB (sc-8051; Santa Cruz), rabbit anti-c-Fos (#06-341; Upstate), rabbit anti-Fra1 (sc-22794; Santa Cruz), mouse anti-Smad2/3 (BD Transduction Laboratories, BD AB, Stockholm, Sweden).

Chromatin immunoprecipitation

Cells were cultured in 10 cm plates to approximately 80–90% confluence, and one plate was used per immunoprecipitation. Cells were fixed with 1% formaldehyde for 10 min at room temperature with swirling. Glycine was added to a final concentration of 0.125 M, and the incubation was continued for an additional 5 min. Cells were washed twice with ice-cold phosphate-buffered saline, harvested by scraping, pelleted and resuspended in 1 ml of SDS lysis buffer (50 mM Tris–HCl (pH 8.0), 1% SDS, 10 mM EDTA, protease inhibitors; complete EDTA-free protease inhibitors (Roche Diagnostics, Rotkreuz, Switzerland)). Samples were sonicated three times for 30 s each time at intervals of 30 s with a Diagenode Bioruptor sonicator. Samples were centrifuged at 14 000 r.p.m. at 8 °C for 10 min. After removal of a control aliquot, supernatants were diluted 10-fold in ChIP dilution buffer (20 mM Tris–HCl (pH 8.0), 150 mM NaCl, 2 mM EDTA, 1% Triton X-100). Samples were incubated at 4 °C overnight in 2-methacryloyloxyethyl phosphorylcholine polymer-treated 15 ml polypropylene tubes (Assist, Tokyo, Japan) with anti-mouse IgG-Dynabeads that had been preincubated with 5 μg of antibodies in phosphate-buffered saline–0.5% bovine serum albumin. The beads were then moved to 1.7 ml siliconized tubes (catalog no. 3207; Corning, Corning, NY, USA) and washed five times with ChIP wash buffer (50 mM HEPES-KOH (pH 7.0), 0.5 M LiCl, 1 mM EDTA, 0.7% deoxycholate, 1% Igepal CA630) and once with TE buffer (pH 8.0). Immunoprecipitated samples were eluted and reverse cross-linked by incubation overnight at 65 °C in elution buffer (50 mM Tris–HCl (pH 8.0), 10 mM EDTA, 1% SDS). Genomic DNA was then extracted with a PCR purification kit (Qiagen, Qiagen Nordic, Sollentuna, Sweden). The immunoprecipitated DNA was analyzed by qPCR assay using specific primers for the human *pai-1* gene: forward, 5′-GCAGGACATCCGGGAGAGA-3′ and reverse, 5′-CCAATAGCCTTGGCCTGAGA-3′; for the human *mmp-10* gene: forward, 5′-AGGCCACTAGGGGGTAGAGCT-3′ and reverse, 5′-AGGCAGAGCAGACTGGCAGACA-3′. The fold enrichment corresponds to the Smad2/3 enrichment in each locus divided first by the enrichment in the negative control regions (*HBB* promoter, *HPRT1* first intron) and then by the IgG control enrichment. Primers for the human β-globin (*HBB*) gene: forward, 5′-AACGTGATCGCCTTTCTC-3′ and reverse, 5′-GAAGCAGAACTCTGCACTTC-3′. Primers for the *HPRT1* gene: forward, 5′-TGTTTGGGCTATTTACTAGTTG-3′ and reverse 5′ ATAAAATGACT TAAGCCCAGAG 3′. Primer design and qPCR conditions were according to the recently published ChIP analysis of Smad-binding at a genome-wide level.[7]

CONFLICT OF INTEREST

UL is a founder of Olink Bioscience, which commercializes the *in situ* PLA technology.

ACKNOWLEDGEMENTS

We thank our colleagues, in particular Aris Moustakas and Masato Morikawa, for their valuable discussion and help with experiments. This work was supported by the Swedish Cancerfonden (090773) and the Netherlands Centre for Biomedical Genetics.

REFERENCES

1 Heldin CH, Moustakas A. Role of Smads in TGFβ signaling. *Cell Tissue Res* 2012; **347**: 21–36.
2 Schmierer B, Hill CS. TGFβ-SMAD signal transduction: molecular specificity and functional flexibility. *Nat Rev Mol Cell Biol* 2007; **8**: 970–982.
3 Zhang Y, Feng XH, Derynck R. Smad3 and Smad4 cooperate with c-Jun/c-Fos to mediate TGF-β -induced transcription. *Nature* 1998; **394**: 909–913.
4 Javelaud D, Mauviel A. Crosstalk mechanisms between the mitogen-activated protein kinase pathways and Smad signaling downstream of TGF-β: implications for carcinogenesis. *Oncogene* 2005; **24**: 5742–5750.
5 Ross S, Hill CS. How the Smads regulate transcription. *Int J Biochem Cell Biol* 2008; **40**: 383–408.
6 Massagué J. TGFβ in cancer. *Cell* 2008; **134**: 215–230.
7 Koinuma D, Tsutsumi S, Kamimura N, Taniguchi H, Miyazawa K, Sunamura M *et al.* Chromatin immunoprecipitation on microarray analysis of Smad2/3 binding sites reveals roles of ETS1 and TFAP2A in transforming growth factor β signaling. *Mol Cell Biol* 2009; **29**: 172–186.
8 ten Dijke P, Arthur HM. Extracellular control of TGFβ signalling in vascular development and disease. *Nat Rev Mol Cell Biol* 2007; **8**: 857–869.
9 Xu J, Lamouille S, Derynck R. TGF-β-induced epithelial to mesenchymal transition. *Cell Res* 2009; **19**: 156–172.
10 Comijn J, Berx G, Vermassen P, Verschueren K, van Grunsven L, Bruyneel E *et al.* The two-handed E box binding zinc finger protein SIP1 downregulates E-cadherin and induces invasion. *Mol Cell* 2001; **7**: 1267–1278.
11 Thuault S, Tan EJ, Peinado H, Cano A, Heldin CH, Moustakas A. HMGA2 and Smads co-regulate SNAIL1 expression during induction of epithelial-to-mesenchymal transition. *J Biol Chem* 2008; **283**: 33437–33446.
12 Zavadil J, Bitzer M, Liang D, Yang YC, Massimi A, Kneitz S *et al.* Genetic programs of epithelial cell plasticity directed by transforming growth factor-β. *Proc Natl Acad Sci USA* 2001; **98**: 6686–6691.
13 Derynck R, Zhang YE. Smad-dependent and Smad-independent pathways in TGF-β family signalling. *Nature* 2003; **425**: 577–584.
14 Mu Y, Gudey SK, Landström M. Non-Smad signaling pathways. *Cell Tissue Res* 2012; **347**: 11–20.
15 Deckers M, van Dinther M, Buijs J, Que I, Löwik C, van der Pluijm G *et al.* The tumor suppressor Smad4 is required for transforming growth factor β-induced epithelial to mesenchymal transition and bone metastasis of breast cancer cells. *Cancer Res* 2006; **66**: 2202–2209.
16 Dzwonek J, Preobrazhenska O, Cazzola S, Conidi A, Schellens A, van Dinther M *et al.* Smad3 is a key nonredundant mediator of transforming growth factor β signaling in Nme mouse mammary epithelial cells. *Mol Cancer Res* 2009; **7**: 1342–1353.
17 Shaulian E, Karin M. AP-1 in cell proliferation and survival. *Oncogene* 2001; **20**: 2390–2400.
18 van Dam H, Castellazzi M. Distinct roles of Jun: Fos and Jun: ATF dimers in oncogenesis. *Oncogene* 2001; 20: 2453–2464.
19 Hess J, Angel P, Schorpp-Kistner M. AP-1 subunits: quarrel and harmony among siblings. *J Cell Sci* 2004; **117**: 5965–5973.
20 Lopez-Bergami P, Lau E, Ronai Z. Emerging roles of ATF2 and the dynamic AP1 network in cancer. *Nat Rev Cancer* 2010; **10**: 65–76.
21 Eferl R, Wagner EF. AP-1: a double-edged sword in tumorigenesis. *Nat Rev Cancer* 2003; **3**: 859–868.
22 Belguise K, Kersual N, Galtier F, Chalbos D. FRA-1 expression level regulates proliferation and invasiveness of breast cancer cells. *Oncogene* 2005; **24**: 1434–1444.
23 Ozanne BW, Spence HJ, McGarry LC, Hennigan RF. Transcription factors control invasion: AP-1 the first among equals. *Oncogene* 2007; 26: 1–10.
24 Wiercinska E, Naber HP, Pardali E, van der Pluijm G, van Dam H, Ten Dijke P. The TGF-β/Smad pathway induces breast cancer cell invasion through the up-regulation of matrix metalloproteinase 2 and 9 in a spheroid invasion model system. *Breast Cancer Res Treat* 2011; **128**: 657–666.
25 Laverty HG, Wakefield LM, Occleston NL, O'Kane S, Ferguson MW. TGF-β3 and cancer: a review. *Cytokine Growth Factor Rev* 2009; **20**: 305–317.
26 Tang B, Vu M, Booker T, Santner SJ, Miller FR, Anver MR *et al.* TGF-β switches from tumor suppressor to prometastatic factor in a model of breast cancer progression. *J Clin Invest* 2003; **112**: 1116–1124.
27 Verde P, Casalino L, Talotta F, Yaniv M, Weitzman JB. Deciphering AP-1 function in tumorigenesis: fra-ternizing on target promoters. *Cell Cycle* 2007; **6**: 2633–2639.
28 Söderberg O, Gullberg M, Jarvius M, Ridderstråle K, Leuchowius KJ, Jarvius J *et al.* Direct observation of individual endogenous protein complexes in situ by proximity ligation. *Nat Methods* 2006; **3**: 995–1000.
29 Baan B, Pardali E, ten Dijke P, van Dam H. *In situ* proximity ligation detection of cJun/AP-1 dimers reveals increased levels of cJun/Fra1 complexes in aggressive breast cancer cell lines *in vitro* and *in vivo*. *Mol Cell Proteomics* 2010; **9**: 1982–1990.

30 Dumont N, Arteaga CL. Transforming growth factor-β and breast cancer: tumor promoting effects of transforming growth factor-β. *Breast Cancer Res* 2000; **2**: 125–132.
31 Wakefield LM, Piek E, Bottinger EP. TGF-β signaling in mammary gland development and tumorigenesis. *J Mammary Gland Biol Neoplasia* 2001; **6**: 67–82.
32 Gomis RR, Alarcon C, Nadal C, Van PC, Massagué J. C/EBPβ at the core of the TGFβ cytostatic response and its evasion in metastatic breast cancer cells. *Cancer Cell* 2006; **10**: 203–214.
33 Levy L, Hill CS. Alterations in components of the TGF-β superfamily signaling pathways in human cancer. *Cytokine Growth Factor Rev* 2006; **17**: 41–58.
34 Sjöblom T, Jones S, Wood LD, Parsons DW, Lin J, Barber TD *et al.* The consensus coding sequences of human breast and colorectal cancers. *Science* 2006; **314**: 268–274.
35 Leary RJ, Lin JC, Cummins J, Boca S, Wood LD, Parsons DW *et al.* Integrated analysis of homozygous deletions, focal amplifications, and sequence alterations in breast and colorectal cancers. *Proc Natl Acad Sci USA* 2008; **105**: 16224–16229.
36 Sundqvist A, ten Dijke P, van Dam H. Key signaling nodes in mammary gland development and cancer: Smad signal integration in epithelial cell plasticity. *Breast Cancer Res* 2012; **14**: 204–216.
37 Parvani JG, Taylor MA, Schiemann WP. Noncanonical TGF-β signaling during mammary tumorigenesis. *J Mammary Gland Biol Neoplasia* 2011; **16**: 127–146.
38 Wagner EF. Bone development and inflammatory disease is regulated by AP-1 (Fos/Jun). *Ann Rheum Dis* 2010; **69**(Suppl 1): i86–i88.
39 Reichmann E, Schwarz H, Deiner EM, Leitner I, Eilers M, Berger J *et al.* Activation of an inducible c-FosER fusion protein causes loss of epithelial polarity and triggers epithelial-fibroblastoid cell conversion. *Cell* 1992; **71**: 1103–1116.
40 Luo YP, Zhou H, Krueger J, Kaplan C, Liao D, Markowitz D *et al.* The role of proto-oncogene Fra-1 in remodeling the tumor microenvironment in support of breast tumor cell invasion and progression. *Oncogene* 2010; **29**: 662–673.
41 Verrecchia F, Tacheau C, Schorpp-Kistner M, Angel P, Mauviel A. Induction of the AP-1 members c-Jun and JunB by TGF-β/Smad suppresses early Smad-driven gene activation. *Oncogene* 2001; **20**: 2205–2211.

Supplementary Information accompanies the paper on the Oncogene website (http://www.nature.com/onc)

A low-grade B-cell lymphoma with prolymphocytic/ paraimmunoblastic proliferation and *IRF4* rearrangement

Translocations between *IRF4* and immunoglobulin genes, present in myeloma[1] and high-grade B-cell lymphomas[2] have not been reported for low-grade B-cell neoplasms. We report 3 low-grade B-cell lymphoma cases with *IRF4* rearrangement showing characteristic morphological features and immunophenotypes.

While checking our laboratory-developed FISH probes for *IRF4* split assay on paraffin sections, we incidentally found *IRF4* rearrangement in case 1 (the sample at recurrence; Figure 1A). The original pathological diagnosis was low-grade B-cell lymphoma, unclassified. The cytogenetic analysis record indicated that this tumor harbored a balanced translocation between the *IGK* and *IRF4* genes, t(2;6)(p11.2;p25). We then performed fusion FISH assays and confirmed *IRF4-IGK* present and *IRF4-IGH* absent (Figure 1B-E). The primary lesion (biopsied eight years prior to the index sample) also displayed *IRF4* rearrangement. A case that had been diagnosed as low-grade B-cell lymphoma, unclassified in the original institute, was presented in a regional pathology conference, ten days after the identification of case 1. The cytomorphological feature of the case was reminiscent of that of case 1 although paraimmunoblasts were more predominant (Figure 1P). The morphology prompted us to perform FISH assays for *IRF4*, obtaining positive results (Figure 1L-O) (case 2). Lymphoma samples (784 cases

Table 1. Clinicopathological summary

		Case 1	Case 2	Case 3
Age at onset/gender		38/F	62/M	66/M
Stage (site of involvement)		Stage 4 (axillary LN, inguinal LN, bone marrow)	Stage 1 (inguinal LN)	Stage 1 (retroperitoneal LN)
White blood count (% lymphocyte)		5.6x10⁹/L (44%)*	5.0x10⁹/L (31%)	6.1x10⁹/L (37%)
International prognostic index		Low	Low	Low
Treatment		For primary lesions: rituximab+CHOP followed by rituximab only. At recurrence (8 years after the initial diagnosis): Rituximab+fludarabine	No treatment (excisional biopsy only)	rituximab+CVP followed by rituximab only
Outcome		Alive with 2nd CR for 10 years after the initial diagnosis	Alive with CR for 1 year after the diagnosis	Alive with CR for 4.5 years after the diagnosis
FISH	*IRF4* split	+	+	+
	IRF4-IGK fusion	+*	ND	ND
	IRF4-IGL fusion	-*	+	ND
	IGK split	+*	-	NE
	IGL split	-*	+	ND
	IGH split	-*	-	ND
	BCL2 split	-*	-	-
	BCL6 split	-*	-	-
	MYC split	-*	-	-
	CCND1 split	-*	-	-
IHC/ISH	CD5	-	-	-**
	CD10	-	-	-
	CD20	+	+	+
	CD23	+	+	+
	CD43	+	+	+
	CD138	-	-	ND
	BCL2	+	+	+
	BCL6	+*	+	+
	MUM1/IRF4	+	+	+
	IgM	+	+	+
	IgD	-*	-	ND
	EBER	-*	-	-
	TdT	-*	-	ND
	Cyclin D1	-	-	-
	Ki67 labeling index	~10%	~10%	~10%
IGHV usage		V3-11*01	V1-8*01	NE
IGHV identity to germline sequence		100%	94.7%	NE
Cytogenetics		46XX,t(2;6)(p11.2;p25)[10]/46XX,t(1;11)(q21;q23)[1]/46XX[9]*	ND	46XY,t(2;6)(p12;p25)[1]/46,sl,-Y,-4,-8,-9,-9,add(11)(q23),+5mar[1]/46XY[11]

LN: lymph node; CHOP: cyclophosphamide+ adriamycin+vincristine+prednisone; CVP: cyclophosphamide+vincristine+prednisone; CR: complete response; FISH: fluorescein in situ *hybridization; IHC/ISH: immunohistochemistry/*in situ *hybridization; ND: not done; NE: not evaluable. *Only data at recurrence were available. ** Dim by flow cytometry.*

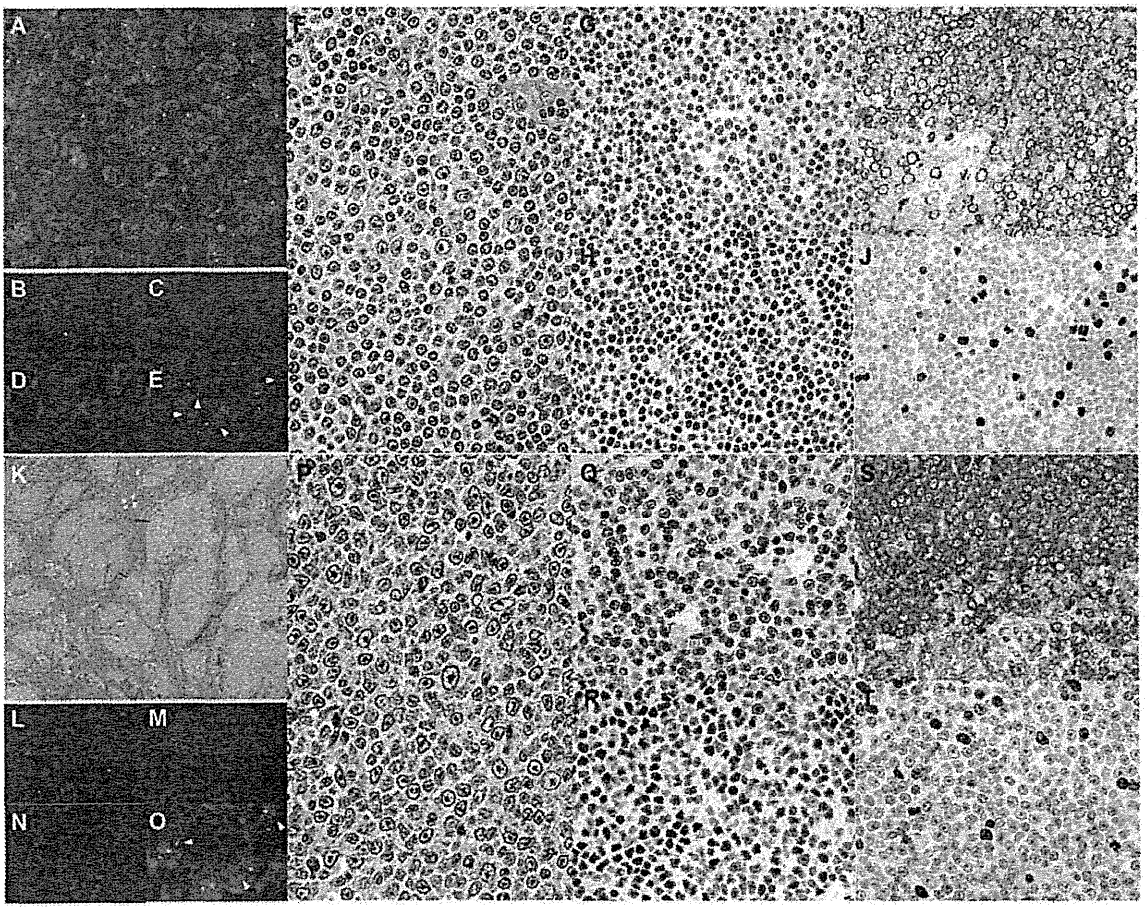

Figure 1. Morphological and histomolecular examination results. Panels A to J and K to T illustrate cases 1 (at recurrence) and 2, respectively. All of the present lesions had positive split FISH assay results for *IRF4*. The lymphoma cells harbored a yellow signal (wild-type *IRF4*) and individual red (5′-side of *IRF4*) and green signals (3′-side of *IRF4*; A). The split FISH assays for *IGK* and *IGL* were positive in cases 1 (B, C, and E) and 2 (L, M, and O), respectively. On the same sections, *IRF4* stained blue (D and N) and was observed fusing to the 3′-side of *IGK* (E, arrowhead) or 3′-side of *IGL* (O, arrowhead). The infiltration pattern was diffuse, but it was divided by sclerotic bands in case 2 (K, 4× objective). The infiltrate comprised prolymphocytes and occasional paraimmunoblasts and small lymphocytes (F, 60× objective). In case 2, paraimmunoblasts were prominent and neoplastic small lymphocytes were rare (P, 60× objective). Most of the lymphoma cells expressed MUM1/*IRF4* (G and Q, 40× objective) and BCL6 (H and R, 40× objective) simultaneously. IgM was strongly expressed (I and S, 40× objective). The Ki67-labeling index was low (J and T, 40× objective).

including 232 low-grade B-cell lymphomas) were screened by split FISH assay for *IRF4*. Case 3 was identified in this process, and the original pathology diagnosis was low-grade B-cell lymphoma, unclassified. The cytogenetic analysis record, t(2;6)(p12;p25), supported the presence of *IRF4-IGK*. Case 1 was also in this cohort and, therefore, 2 of 232 low-grade B-cell lymphomas (0.86%) harbored *IRF4* rearrangement in the cohort.

Histologically, the infiltrate was basically diffuse, and the lymph node architecture was totally effaced. In case 2, however, broad fibrotic bands divided the lymphoma infiltrate into nodules (Figure 1K). The lymphoma cells in the 4 lesions from the 3 patients comprised prolymphocytes, paraimmunoblasts, and small lymphocytes, varying in proportion between lesions. No proliferation centers or lymph follicles were seen, except for the primary lesion in case 1, in which areas of prolymphocytic and paraimmunoblastic infiltration were confluent with a background of neoplastic small lymphocytes and a few regressed primary follicles without follicular colonization were highlighted by the presence of follicular dendritic cell (FDC) network as determined by anti-CD23 immunohistochemistry. In case 1, the recurring lesion showed a diffuse infiltrate of prolymphocytes and occasional paraimmunoblasts (Figure 1F). In case 2, most tumor cells were paraimmunoblasts admixed with occasional prolymphocytes (Figure 1P). On morphological examination only, this cytomorphological feature, together with fibrotic nodularity (Figure 1K), might lead to a differential diagnosis of grade 3 follicular lymphoma (FL). However, these nodules had no FDC networks. Case 3 comprised prolymphocytes and small-to-medium cells with a small central nucleolus in an irregular nucleus (giving an impression of mantle cell lymphoma, MCL), but it was somewhat indefinite because of admixed T cells and tissue scarcity. The immunohisto-

chemical results for the 3 cases indicated CD5$^-$ (dim in case 3 by flow cytometry), CD10$^-$, CD20$^+$, CD23$^+$, CD43$^+$, CD138$^-$, MUM1/*IRF4*$^+$ (Figure 1G and Q), BCL2$^+$, BCL6$^+$ (Figure 1H and R), IgM$^+$ (Figure 1I and S), IgD$^-$, TdT$^-$, and Cyclin D1$^-$. LMO2 was negative in cases 1 and 2 (occasional lymphoma cells were positive in the latter) (*Online Supplementary Figure S1*). The Ki67-labeling index was universally low (approximately 10%; Figure 1J and T). The clinical courses and the results of FISH analyses are summarized in Table 1.

The overall histological impression of the present cases is reminiscent of chronic lymphocytic leukemia/small lymphocytic lymphoma (CLL/SLL) with prominent prolymphocytic/paraimmunoblastic infiltration (the tumor-forming subtype of CLL/SLL[3,4] or paraimmunoblastic variant of CLL/SLL[5-8]) or tissue involvement of B-cell prolymphocytic leukemia (B-PLL). We examined cases 1 and 2 for 4 chromosomal aberrations, which are commonly observed in CLL/SLL [del(11)(q22.3), +12, del(13)(q14.3) del(17)(p13.1)] by FISH, and LEF1, which is characteristically expressed in CLL/SLL,[9] by immunohistochemistry. All were negative in case 2, but 13q14.3 was deleted and LEF1 was weakly expressed in case 1 (*Online Supplementary Figure S2*), implying that case 1 might be more closely related to CLL/SLL.

In CLL/SLL, small lymphocytes are negative or only faintly positive for MUM1/ *IRF4* and BCL6 expression, whereas prolymphocytes and paraimmunoblasts are moderately positive for MUM1/*IRF4* but negative for BCL6.[10,11] In contrast, most lymphoma cells in the present cases expressed MUM1/*IRF4* and BCL6, an uncommon characteristic of well-known low-grade B-cell lymphomas. The cases reported as paraimmunoblastic variants of CLL/SLL were positive for CD5, followed an aggressive clinical course, and harbored *IGH-CCND1* (5 of 8 examined cases).[5-8] These features suggest that most of the reported cases represented MCL (especially pleomorphic variant). None of the present cases showed any aggressive clinical behavior and they showed *IRF4* rearrangement without other translocations commonly observed in B-cell neoplasms including *CCND1* rearrangement. Variable expression of CD5, strong expression of IgM, and absence of IgD in the present cases are not typical in CLL/SLL and may be suggestive of the immunophenotype of B-PLL. However, none of our patients showed leukemic involvement of the peripheral blood and *IRF4* rearrangement has not been reported in B-PLL. Nodal involvement by B-PLL is rare, and previous histological studies probably included MCL.[12] The morphological features, immunophenotype, genetics, and clinical presentation of the present cases seemed incompatible with those of existing subtypes, prompting us to distinguish the present cases as "prolymphocytic/ paraimmunoblastic lymphoma (PPL)". The relationship with other low-grade B-cell neoplasms remains to be clarified.

The question of whether the present cases are 'precursors' of the *IRF4*-rearranged high-grade B-cell lymphomas[2] remains unanswered. Cytogenetic analyses were successful in case 1, 46XX,t(2;6)(p11.2;p25)[10]/46XX,t(1;11)(q21;q23)[1]/46XX[9], and case 3, 46XY,t(2;6)(p12;p25)[1]/46,sl,-Y,-4,-8,-9,-9,add(11)(q23),+5mar[1]/46XY[11]. No evidence of rearrangement in *BCL2*, *BCL6*, *MYC*, and *CCND1* was obtained in the present cases, whereas in previous cases,[2] 7 and 1 of the 19 *IRF4*-rearranged high-grade B-cell lymphomas showed *BCL6* and *MYC* rearrangements, respectively. PCR for IGH gene rearrangement was successful in cases 1 and 2. The *IGHV* usage was V3-11*01 and V1-8*01, and identity to germline sequences from CDR1 to FWR3 regions was 100% and 94.7%, respectively, with intraclonal diversity in the latter. These mutation statuses may contrast to those in the *IRF4*-rearranged high-grade B-cell lymphomas (93.9%-86.1%).[2] Light-chain genes were the translocation partners of *IRF4* in the present cases and IGH in 17 of the 19 *IRF4*-rearranged high-grade B-cell lymphoma cases studied by Salaverria *et al.*[2] (P=0.0065, Fisher's exact test). Most patients with high-grade cases were young,[2] indicating that *IRF4*-rearranged high-grade B-cell lymphomas are likely to be *de novo*. However, it is interesting that case 15 in the series of Salaverria *et al.*[2] harbored *IGK* as its *IRF4* partner and was a transformed lymphoma.[2] The present and previous findings indicate that *IRF4* rearrangement may be related to the development of low-grade and primary high-grade lymphomas and that some *IRF4*-rearranged low-grade lymphomas may progress to high-grade lymphomas.

To clarify the questions presented here, more "PPL" cases should be examined. The prolymphocytic/paraimmunoblastic morphological features and co-expression of BCL6 and MUM1/*IRF4* in most lymphoma cells are key indications for confirmatory FISH for *IRF4* rearrangement.

Kengo Takeuchi,[1,2] Seiji Sakata,[1] Reimi Asaka,[1,2] Naoko Tsuyama,[2] Akito Dobashi,[1] Masaaki Noguchi[3]

[1]Pathology Project for Molecular Targets; [2]Division of Pathology, The Cancer Institute, Japanese Foundation for Cancer Research, Tokyo; [3]Department of Hematology, Urayasu Hospital, Juntendo University, Chiba, Japan

Correspondence: kentakeuchi-tky@umin.net

doi:10.3324/haematol.2012.076851

Key-words: B-cell lymphoma, prolymphocytic, paraimmunoblastic, IRF4 rearrangement.

Acknowledgments: we thank Drs. Sheng-Tsung Chang, Masahiro Yokoyama, Yasuhito Terui and the members of the Ganken Ariake Lymphoma Study Group (GALSG) and Tokyo Lymphoma Study Group (TLSG) for their advice. We thank Ms. Satoko Baba and Ms. Noriko Matsumoto for their technical assistance. We also thank Ms. Sayuri Sengoku for her administrative assistance. This study was supported in part by Grants-in-Aid for Scientific Research from the Ministry of Education, Culture, Sports, Science and Technology, Japan, and by grants from the Japan Society for the Promotion of Science, Ministry of Health, Labor, and Welfare of Japan, Vehicle Racing Commemorative Foundation of Japan, and Izumo City Supporting Cancer Research Project.

Information on authorship, contributions, and financial & other disclosures was provided by the authors and is available with the online version of this article at www.haematologica.org.

References

1. Iida S, Rao PH, Butler M, Corradini P, Boccadoro M, Klein B, et al. Deregulation of MUM1/IRF4 by chromosomal translocation in multiple myeloma. Nat Genet. 1997;17(2):226-30.
2. Salaverria I, Philipp C, Oschlies I, Kohler CW, Kreuz M, Szczepanowski M, et al. Translocations activating IRF4 identify a subtype of germinal center-derived B-cell lymphoma affecting predominantly children and young adults. Blood. 2011;118 (1):139-47.
3. Lennert K, Feller AC. Histopathology of Non-Hodgkin's Lymphomas (Based on Updated Kiel Classification). 2nd ed. New York: Springer-Verlag, 1992.
4. Lennert K. Malignant Lymphomas. Berlin: Springer-Verlag, 1978.
5. Espinet B, Larriba I, Salido M, Florensa L, Woessner S, Sans-

Sabrafen J, et al. Genetic characterization of the paraimmunoblastic variant of small lymphocytic lymphoma/chronic lymphocytic leukemia: A case report and review of the literature. Hum Pathol. 2002;33(11):1145-8.
6. Frater JL, Tsiftsakis EK, Hsi ED, Pettay J, Tubbs RR. Use of novel t(11;14) and t(14;18) dual-fusion fluorescence in situ hybridization probes in the differential diagnosis of lymphomas of small lymphocytes. Diagn Mol Pathol. 2001;10(4):214-22.
7. Grosso LE, Kelley PD. bcl-1 translocations are frequent in the paraimmunoblastic variant of small lymphocytic lymphoma. Mod Pathol. 1998;11(1):6-10.
8. Pugh WC, Manning JT, Butler JJ. Paraimmunoblastic variant of small lymphocytic lymphoma/leukemia. Am J Surg Pathol. 1988;12(12):907-17.
9. Tandon B, Peterson L, Gao J, Nelson B, Ma S, Rosen S, et al. Nuclear overexpression of lymphoid-enhancer-binding factor 1 identifies chronic lymphocytic leukemia/small lymphocytic lymphoma in small B-cell lymphomas. Mod Pathol. 2011;24(11):1433-43.
10. Falini B, Fizzotti M, Pucciarini A, Bigerna B, Marafioti T, Gambacorta M, et al. A monoclonal antibody (MUM1p) detects expression of the MUM1/IRF4 protein in a subset of germinal center B cells, plasma cells, and activated T cells. Blood. 2000;95(6):2084-92.
11. Falini B, Fizzotti M, Pileri S, Liso A, Pasqualucci L, Flenghi L. Bcl-6 protein expression in normal and neoplastic lymphoid tissues. Ann Oncol. 1997;8(2 Suppl):101-4.
12. Swerdlow SH, Campo E, Harris NL, Jaffe ES, Pileri SA, Stein H, et al. eds. WHO classification of Tumours of Haematopoietic and Lymphoid Tissues. Lyon: IARC Press, 2008.